Molecular mechanism of ectodermal patterning in *Xenopus laevis*

Tomoko Kurata

DOCTOR OF PHILOSOPHY

DEPARTMENT OF MOLECULAR BIOMECHANICS
SCHOOL OF LIFE SCIENCE
THE GRADUATE UNIVERSITY FOR ADVANCED STUDIES

2002

CONTENTS

GENERAL INTRODUCTION

During the process of neurulation in vertebrates, the ectoderm is differentiated into several distinct tissue types including neural plate, epidermis, and neural crest (Fig.0). Recent works, mainly in *Xenopus*, have focused upon molecular mechanisms that can direct ectoderm to neural fates. In the models, neural induction is initially caused by inhibition of BMP activities in ectoderm by secreted BMP antagonists *Noggin*, *Chordin* and *Follisitatin* that induced in Spemann's organizer. Dorsal ectoderm that has low BMP signaling differentiated into neural plate and ventral ectoderm that has high BMP signaling differentiated into epidermis. However, neural crest induction is more complicated. Neural crest is induced at the border between prospective neural plate and prospective epidermis. Molecular embryological studies have indicated that several secreted molecules are involved in the neural crest induction. One model suggests that an intermediate level of BMP signalling that is generated by the balance between the BMPs and BMP antagonists plays a role in establishing the neural crest fate in *Xenopus* and Zebrafish (Barth et al., 1999; Marchant et al., 1998). It was also reported that canonical Wnt signaling and fibroblast growth factor (FGF) signaling enhances neural crest induction, cooperating with BMP antagonists (LaBonne and Bronner-Fraser, 1998; Mayor et al., 1997). Several transcriptional factors that able to induced neural crest makers such as *Zic*-related genes were reported (Mizuseki et al., 1998; Nakata et al., 2000; Nakata et al., 1997; Nakata et al., 1998). But many of them can also induce neural plate makers and they are expressed in not only theneural crest region but also in the neural plate. Positioning mechanisms of neural-epidermal border and mechanisms of neural crest induction are poorly understood. Thus, it is complicated to understand how

to diverge neural plate and neural crest fates.

In order to understand of molecular mechanisms of ectodermal patterning, I first focused on the *in vivo* BMP activity that is a basis of the neural and epidermal induction. I performed visualization of the endogenous BMP signaling using an antibody that preferentially recognizes the BMP-stimulated form of Smads, and reviewed roles of BMP activities that were suggested by previous studies in chapter 1. Furthermore, I also demonstrated *Nbx,* a novel homeobox gene may be essential for rigorous regional specification on neural-epidermal border and neural crest induction in the downstream process of pattern formation by BMP activity in chapter 2.

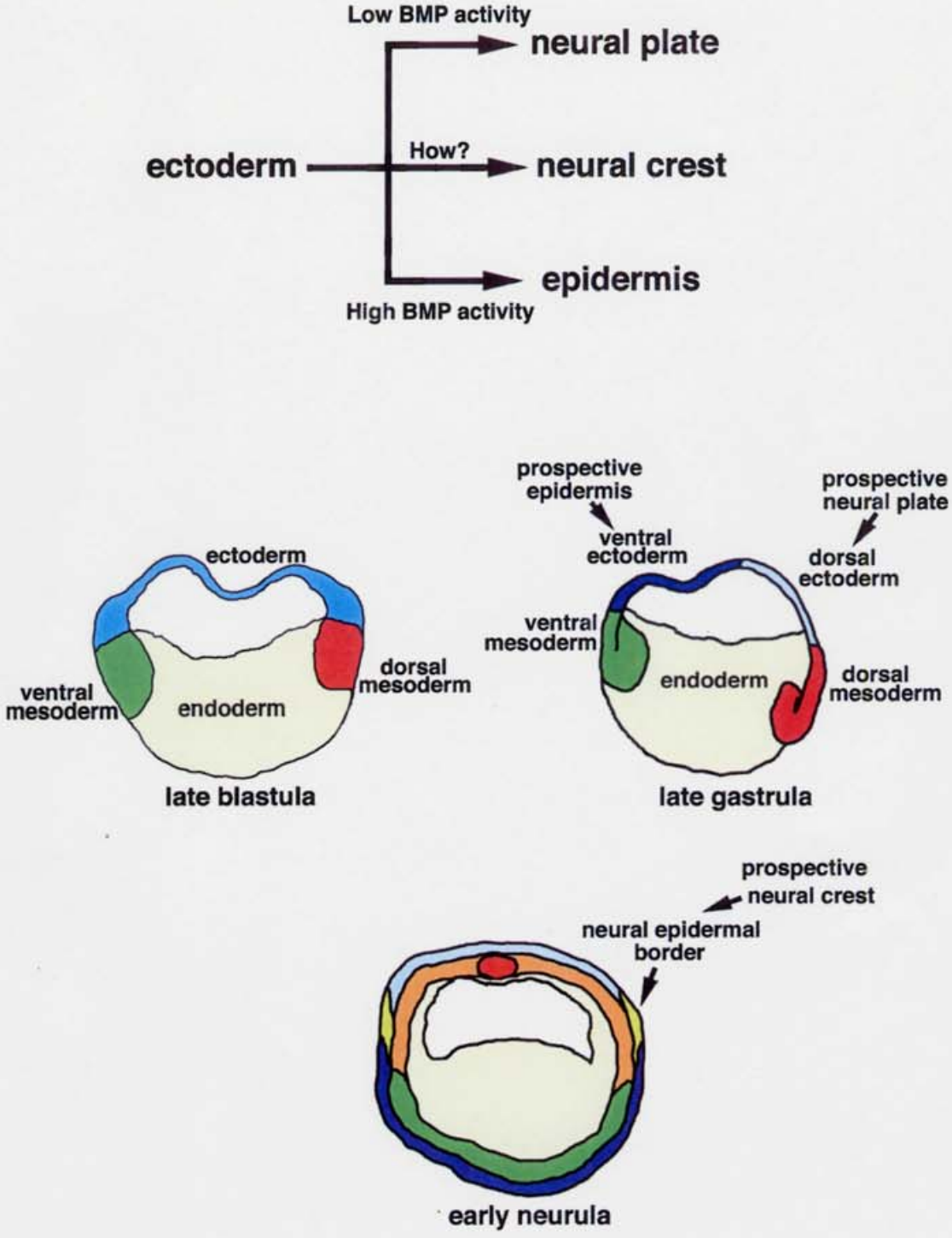

Fig.0 Ectodermal patterning in *Xenopus*

CHAPTER 1

Visualization of endogenous BMP signaling during *Xenopus* development

Summary

Here I showed the pattern of endogenous BMP activity during ectodermal patterning. The TGF-β superfamily is known to transmit signals to the nucleus mainly through the Smads, intracellular signaling components that are highly conserved from nematodes to humans. The signaling activity of the Smads is regulated by their ligand-stimulated phosphorylation through Ser/Thr kinase receptors. I investigated the spatio-temporal activation of BMP-regulated signals during *Xenopus* development, using a polyclonal antibody that specifically recognizes the phosphorylated form of BMP-regulated Smads. BMP signaling was observed uniformly in early blastula, but was restricted to the ventral side of the embryo from the late blastula stage. At gastrula prospective neural plate region and dorsal mesoderm region were less stained. These results supporting the proposed roles of BMPs as ventralizing factors and anti-neurulizing factors in *Xenopus* embryos. From late neurula BMP signaling was detected at dorsal part of the neural tube and neural crest cells. This results supporting the proposed roles of BMPs as dorsalizing factors in the neural tube. Moreover I showed the BMP activity during eye formation. My observation provides useful information that supports the in vivo roles of BMP activity that were suggested by previous studies.

Introduction

Bone morphogenetic proteins (BMPs) belonging to the transforming growth factor beta (TGF-β) superfamily regulate the differentiation of a variety of cell types, pattern formation in early embryos, and organogenesis (Hogan, 1996). These activities are mediated by receptor Ser/Thr kinases and intracellular signaling components, including Smads (Fig.1-1). BMP-related signals are mediated by Smad1, Smad5, Smad8, and activin/nodal/Vg1-related signals are mediated by Smad2 and Smad3. In addition to these pathway-restricted Smads, a common Smad, Smad4, is required for the nuclear translocation of Smads and for transcriptional activation. The target genes then execute further sequential molecular events (Massague and Wotton, 2000). Extensive studies using *Xenopus* embryos have revealed that some target genes are induced by ligands of TGF-β superfamily in a dose-dependent manner; that is, different set of genes are induced at different concentrations of activin or BMP (Dosch et al., 1997; Dyson and Gurdon, 1998; Wilson et al., 1997). The dose-dependent target gene activation suggests that the ligands of TGF-β superfamily could serve as molecular cues to establish a morphogen gradient. In *Drosophila*, Dpp, the homologue of BMP2/4 that is expressed dorsally, is proposed to act as a morphogen for embryo patterning by specifying the dorsal ectoderm (Irish and Gelbart, 1987). To prove this, a graded distribution of Dpp protein needs to be demonstrated. However, the detection of endogenous levels of BMP/Dpp proteins in embryonic and adult tissues is hampered by the lack of sensitive antibodies against BMP ligands. This lack is probably due to a low immunogenicity of mature BMP ligand proteins, whose amino acid sequences are highly conserved among species. Therefore, it has not been possible to determine the exact range of ligand distribution for BMP2 and BMP4. Moreover, ligand distribution may not correlate with

the actual gradient of morphogen activity, considering the presence of negative regulators, such as *Noggin*, *Chordin*, and *Follistatin*, in the case of the BMPs (Dale and Jones, 1999). Furthermore, signaling system composed of BMP ligands and their receptors, and downstream target genes are complex. And therefore it is quite difficult to evaluate BMP signals by analyzing BMP target genes. A preferred method to evaluate BMP signaling *in situ* is to detect activated forms of intracellular signaling molecules specific for BMP. Smads 1, 5, and 8 are best characterized signaling components of BMP signals and believed to be mediating a major part, if it is not all, of BMP activity. DPP activity has been successfully monitored by visualizing the activated form of Mad, a fly homolog of vertebrate Smad1 (Tanimoto et al., 2000).

In this study, I attempted to localize the sites in developing *Xenopus* embryos where BMP-related signals are transduced abundantly, using an antibody that preferentially recognizes a BMP-stimulated form of Smad (Fig.1-1). My observation provides useful information that supports the in vivo roles of BMP activity during ectodermal patterning that suggested by previous studies.

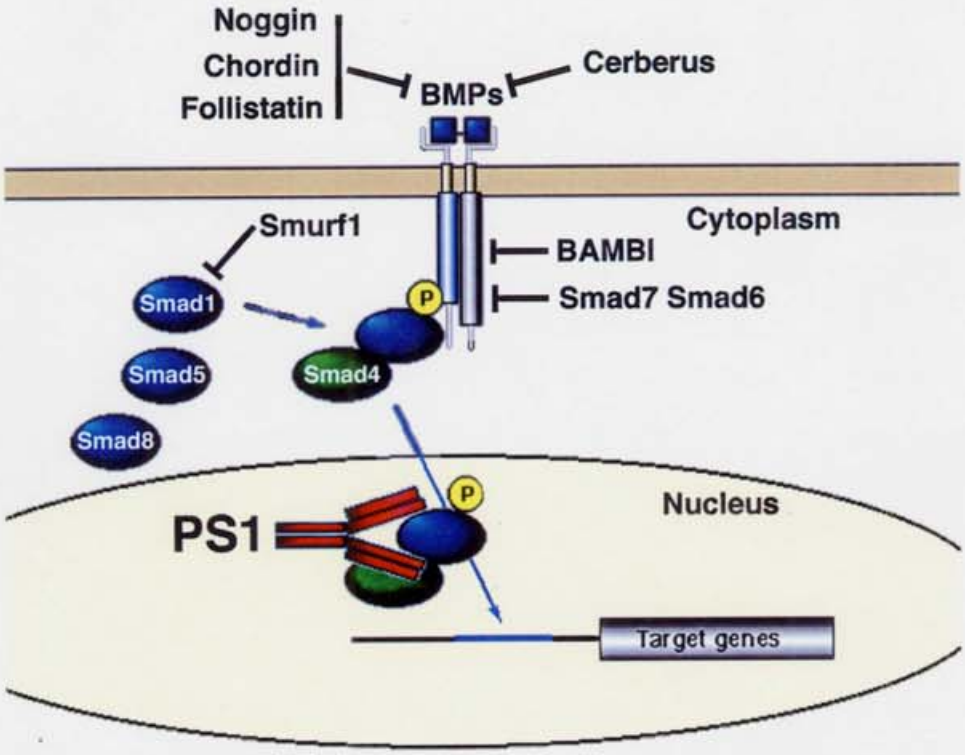

Fig.1-1 BMP signalling

Ligand binding leads to activation of BMP receptors. Activated receptors lead to phosphorylation and activation of Smad1. Smad1 then form complexes of Smad4. Activated Smad complexes are recruited to DNA. The pathway is further regulated at different points as shown. Ligand antagonists (Noggin, Chordin, Follistatin and Cerberus) function extracellularly, preventing ligand binding to the receptor. The pseudoreceptor BAMBI is incorporated into receptor complexes but dose not signal. Inhibitory Smads (Smad6 and Smad7) can act at the level of the receptors or in the case of Smad6, can also compete with Smad4 for activated Smad1. Smurf1 is E3 ubiquitin ligase that targets Smad1 for degradation.

PS1 antibody recognizes phosphorylated Smad1, 5, 8.

Results and Discussion

Specificity of Antibody

In this study, I used a polyclonal antibody, PS1, which was raised against a phosphorylated peptide corresponding to the amino acid sequence of Smad1 that includes the SSXS motif (Persson et al., 1998). PS1 recognizes the phosphorylated, but not the unphosphorylated form of Smad1, Smad5, and Smad8 (Faure et al., 2000; Persson et al., 1998). I examined the ability of PS1 to detect endogenous *Xenopus* Smad proteins activated by BMP-related ligands by Western blotting (Fig.1-2 A). Animal caps dissected from stage 8.5 uninjected embryos, embryos injected with mRNA for BMP4 (50 pg) or embryos injected with mRNAs for both BMP4 (50 pg) and a dominant-negative BMP type IA receptor (DN-BMPR IA, 500 pg), were analyzed by Western blotting with PS1. Specific bands migrated at approximate 67 kDa were detected in both uninjected animal cap and animal cap injected with BMP4 but not in animal cap injected with both BMP4 and DN-BMPR IA. The intensity of the bands was much enhanced by BMP4 overexpression. These results supported that PS1 recognizes phosphorylated forms of *Xenopus* Smads activated by BMP4 signaling. The major components of the bands recognized by PS1 are mostlikely to be *Xenopus* Smad1, although I could not exclude the possibility that the bands detected in the Western blotting includes Smad5 and/or Smad8 that have not been identified in *Xenopus* so far. Detection of the specific bands in the uninjected animal cap showed that PS1 could detect endogenous level of Smad phosphorylation.

I then examined which whether PS1 could detect in situ activation of Smads in

Xenopus embryos by microinjecting mRNAs for each of the BMP-related ligands into the animal pole at the 2-cell stage, followed by whole-mount fixation and immunostaining. The stage-9 embryo stained with unimmunized control serum did not show the nuclear staining (Fig.1-2 B) and embryo stained with PS1 shows the specific nuclear staining (Fig.1-2 C). If mRNA for BMP2, BMP4 or BMP7 was injected, intense nuclear staining was observed in stage-8.5 embryo (Fig.1-2 E, F, G). Activin, which is known to drive Smad2/3 activation, did not increase the staining (Fig.1-2 H). Importantly, I am able to detect nuclear staining in untreated control embryos, suggesting that PS1 is sensitive enough to detect an endogenous level of BMP-like activity histochemically (Fig.1-2 C, D). This was also supported by the observation of ventrally localized staining of intact embryos, described below (Fig.1-3 D). Inhibition of BMP signals by the overexpression of a DN-BMPR IA resulted in decreased staining that was below background levels, further supporting the idea that the staining was specific for endogenous BMP signaling (Fig.1-2 I). Likewise, the nuclear staining induced by overexpressing exogenous ligands was abolished by co-expression with DN-BMPR IA (Fig.1-2 J).

These results establish the usefulness of this antibody as a tool for visualizing the level of BMP-stimulated signaling in early embryos and tissues.

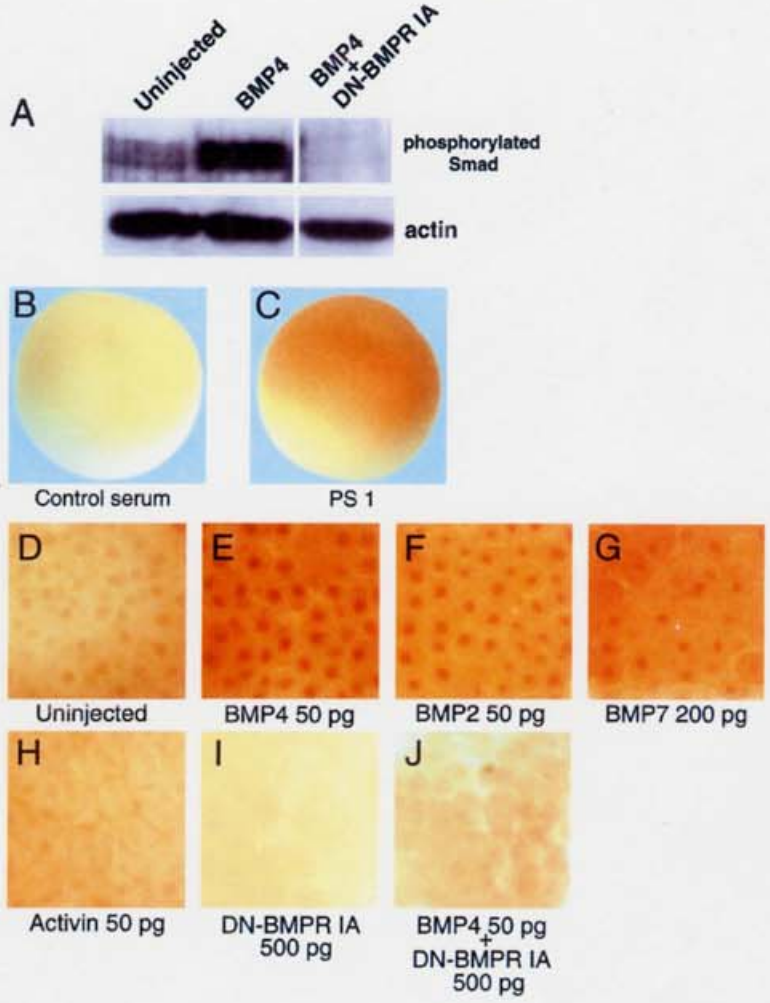

Fig.1-2 Specificity of PS1 antibody

Specificity of PS1 antibody was analysed by Western blotting and immunohistochemistry. **A:** Embryos were injected with mRNAs at the 2-cell stage into the animal pole, and the animal caps at stage 8.5 were analyzed by Western blotting with PS1 antibody. Uninjected embryos (Un), injected with 50pg of BMP4 mRNA (BMP4), co-injected with 50pg of BMP4 and 500pg of DN-BMPR IA (BMP4 + DN-BMPR IA). Blots were reprobed with anti-action antibody as internal control. **B, C:** Embryos were stained with unimmunized control serum (**B**) or PS1 antibody (**C**) at stage 9. **D-J:** Embryos were injected with mRNAs at the 2-cell stage into the animal pole, and stained with PS1 antibody at stage 8.5. The animal hemisphere of control (uninjected) embryo (**D**), injected with 50pg of BMP4 mRNA (**E**), 50pg of BMP2 mRNA (**F**), 200pg of BMP7 mRNA (**G**), 50pg of Activin b B mRNA (**H**), 500pg of DN-BMPR IA (**I**), and coinjected with 50pg of BMP4 mRNA and 500pg of DN-BMPR IA (**J**).

BMP activity in blastula

The staining of embryos at different stages with PS1 revealed that phosphorylation and nuclear translocation of Smads occur as early as stage 7, without any indication of a dorso-ventral difference (Fig.1-3 A). The nuclei of almost all blastomeres except for several cells at the most vegetal region were stained at this stage (Fig.1-3 B, C). This stage is just before the mid-blastula transition (MBT) takes place, and this result shows that BMP-like signaling occurs even before the initial expression of zygotic BMP4. Therefore, PS1 staining at stage 7 should be induced by other ligands such as BMP2 and BMP7, transcripts of which were reported to be present in early *Xenopus* embryo maternally (Hawley et al., 1995; Nishimatsu et al., 1992).

It is well accepted that ventrally expressed BMP4 is responsible for the ventralization of the early *Xenopus* gastrula embryo (Graff et al., 1994; Suzuki et al., 1994). In zebrafish, a dorsalized mutant, *swirl*, was found to result from a mutation of *bmp-2*, demonstrating that at least BMP2 serves as an endogenous ventralizing factor (Kishimoto et al., 1997). Thus, BMP activity is expected to be asymmetrically distributed along the DV axis and more abundant in the ventral hemisphere in early embryos. In fact, in stage-9 embryos, before the onset of gastrulation, and the zygotic expression of BMP is known to begin, the staining became weaker in the dorsal side (Fig.1-3 D). Intense staining was observed in animal, equatorial, and vegetal cells of the ventral side, while weak staining was seen in the most dorsal side of the embryo. In the equatorial region, the ventral three quarters was stained, but the dorsal quarter was not (Fig.1-3 F). At this stage, the BMP antagonists noggin, chordin, and follistatin start to be expressed in the organizer region. Therefore, the dorsal decrease of BMP signaling may be caused by the effect of the

BMP antagonists. Alternatively, BMP activity may be suppressed even before these organizer genes are expressed, by other mechanisms such as Wnt signaling (Baker et al., 1999). The down regulation of BMP activity in the presumptive dorsal lip observed in this study is the earliest indication of blastopore formation and the establishment of the Spemann's organizer. Specification map was illustrated schematically in Fig.1-3 E.

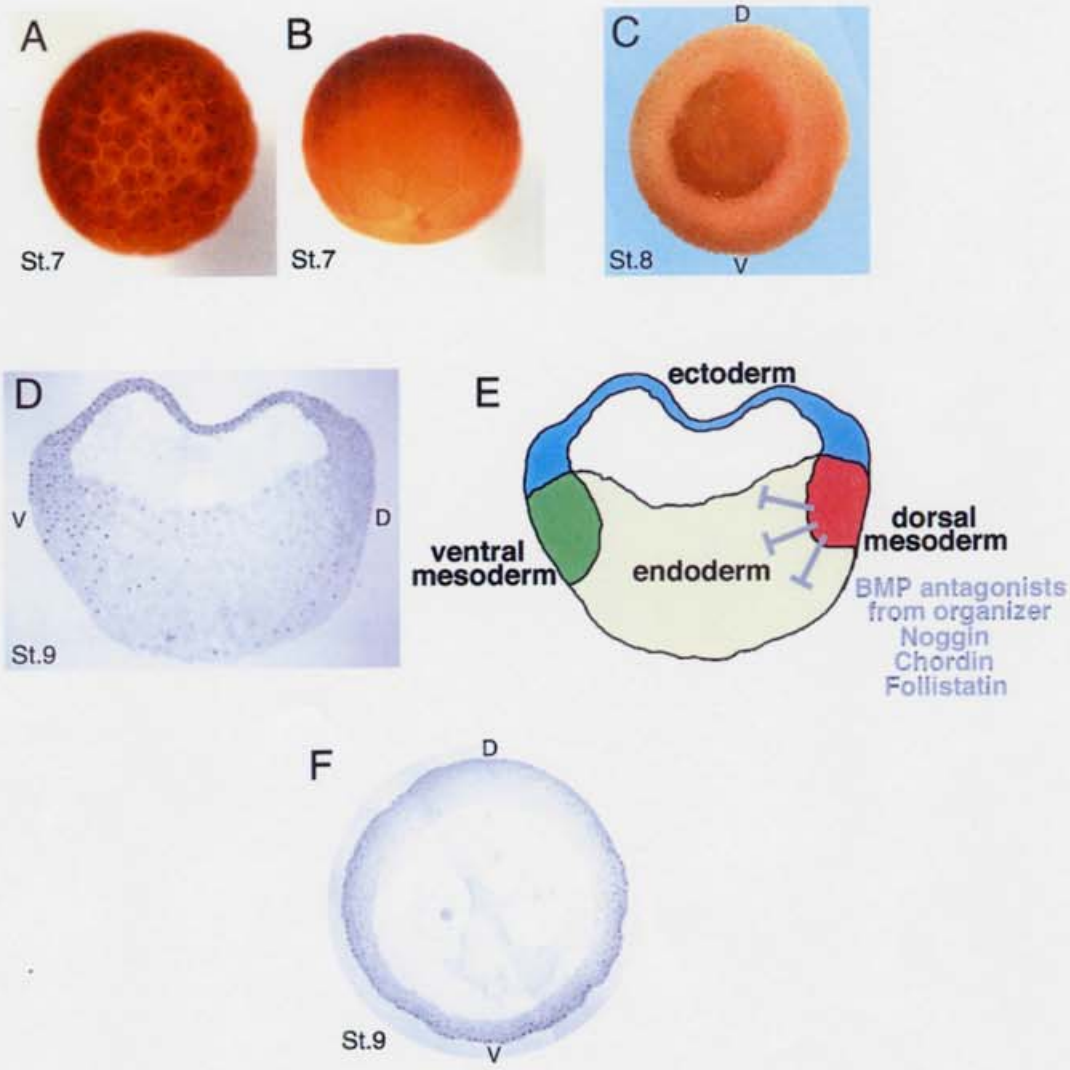

Fig.1-3 PS1 staining pattern in blastula

Xenopus blastula-stage embryos were stained with PS1 antibody. **A, B:** Animal (**A**) and lateral (**B**) view of whole-mount-stained and cleared embryos at stage 7. **C:** Horizontally sectioned surface through the equator at stage 8. **D-H:** Sectioned embryos along D-V axis at stage 9 (**D**). **E:** Horizontally sectioned stage-9 embryo through the equatorial region. Specification map was illustrated schematically in **E**.
(D, dorsal side; V,ventral side)

BMP activity in gastrula

At stage 10, The PS1 staining becomes weaker in the presumptive neural ectoderm and involuting dorsal mesoderm (Fig.1-4 A). This result is consistent with a recent report by Faure et al. (Faure et al., 2000). It was most likely due to the negative regulation of BMP activity by BMP antagonists secreted from the organizer, therefore BMP4 expression, which is sustained by auto-regulation, may be significantly reduced. At this stage, the presumptive anterior endomesoderm was less stained, probably due to the presence of another type of BMP antagonist, *Cerberus*, which is expressed in this region (Piccolo et al., 1999). In contrast, intense staining was seen in the ventral vegetal cells, suggesting that BMP plays a role in ventral endoderm specification. Specification map was illustrated schematically in Fig.1-4 B.

In stage 11-embryos, a gradient of PS1 staining becomes evident in the dorsal ectoderm, along the anterior-posterior axis (Fig.1-4 C). This gradient could be generated either by BMP ligand diffusing from the ventral region, or by negative regulators diffusing from the organizer. Because the observations in *Xenopus* (Ohkawara et al., 2002) and in zebrafish (Nikaido et al., 1999) suggest that at least BMP2 and BMP4 cannot act over a long distance and only inefficiently form gradients by diffusion in the ectodermal cell layer, the latter may be the case. In any case, this is the first observation of a graded level of BMP signaling in a vertebrate embryo.

As gastrulation proceeded, the less stained region increasingly expanded to the anterior region. The anterior border of the stained region overlapped with the presumptive cement gland region (Fig.1-4 D). The cement gland forms between the

anteriormost epidermis and the neural region. It has previously been proposed that the cement gland is induced by an intermediate level of BMP activity (Gammill and Sive, 2000; Wilson et al., 1997). My results indicate the presence of graded BMP signaling in this region which would support this hypothesis.

I measured the staining intensity of nucleus in dorsal ectodermal cells by NIH image (Fig.1-4 E). The mean values of each boxed region were shown in Fig.1-4 F.

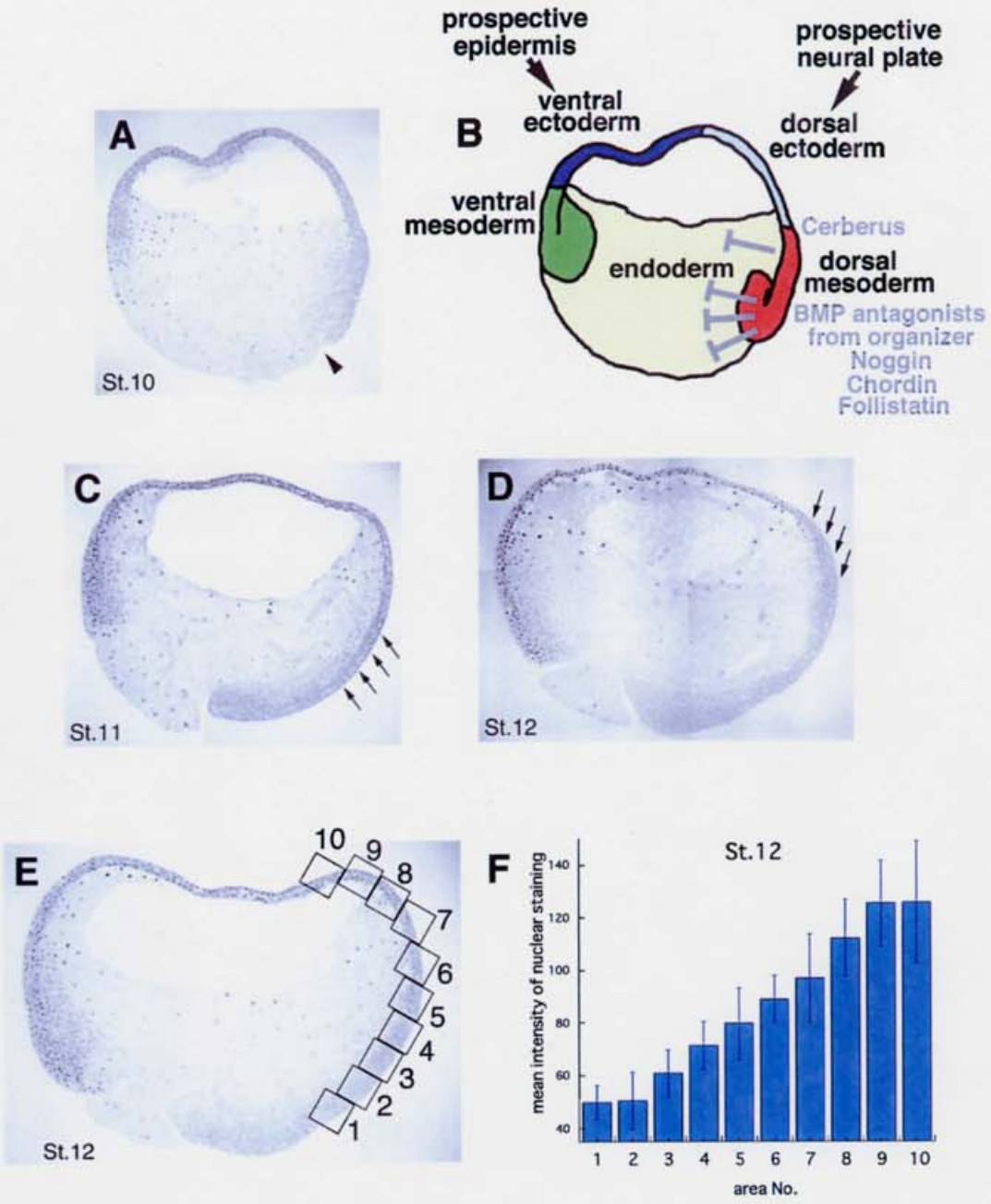

Fig.1-4 PS1 staining pattern in gastrula

Xenopus gastrula-stage embryos were stained with PS1 antibody.

A, C, D: Sectioned embryos along D-V axis at stage 10 (**A**), stage 11 (**C**), stage 12 (**D**). Specification map at stage 10 was illustrated schematically in **B**. **E, F:** Gradient of PS1 staining in the dorsal ectoderm. The staining intensity of each nucleus in the dorsal ectodermal cells in **E** was measured by NIH image and mean values of each boxed region were calculated. Error bars in **F** show +- standard deviation.

BMP activity during the neural crest induction

The most ventral parts of the ectoderm, mesoderm, and endoderm appeared to receive a high level of BMP signaling at early neurula (Fig.1-5 G). This ventral staining was gradually reduced along the DV axis in all three germ layers, towards the dorsalmost region of the embryo, again indicating the presence of a BMP signaling gradient. It was illustrated schematically in Fig.1-5 H. In *Xenopus*, the partial or incomplete inhibition of BMP activity induces the neural crest marker *Slug* in animal cap explants (Marchant et al., 1998). My observation may support at least the existence of medium BMP activity at neural-epidermal border in *Xenopus*. Because many other signaling molecules, including Wnt and FGF are thought to be involved in neural crest formation (LaBonne and Bronner-Fraser, 1998; Mayor et al., 1997), a medium range of BMP activity is not likely to be the only mechanism inducing the neural crest.

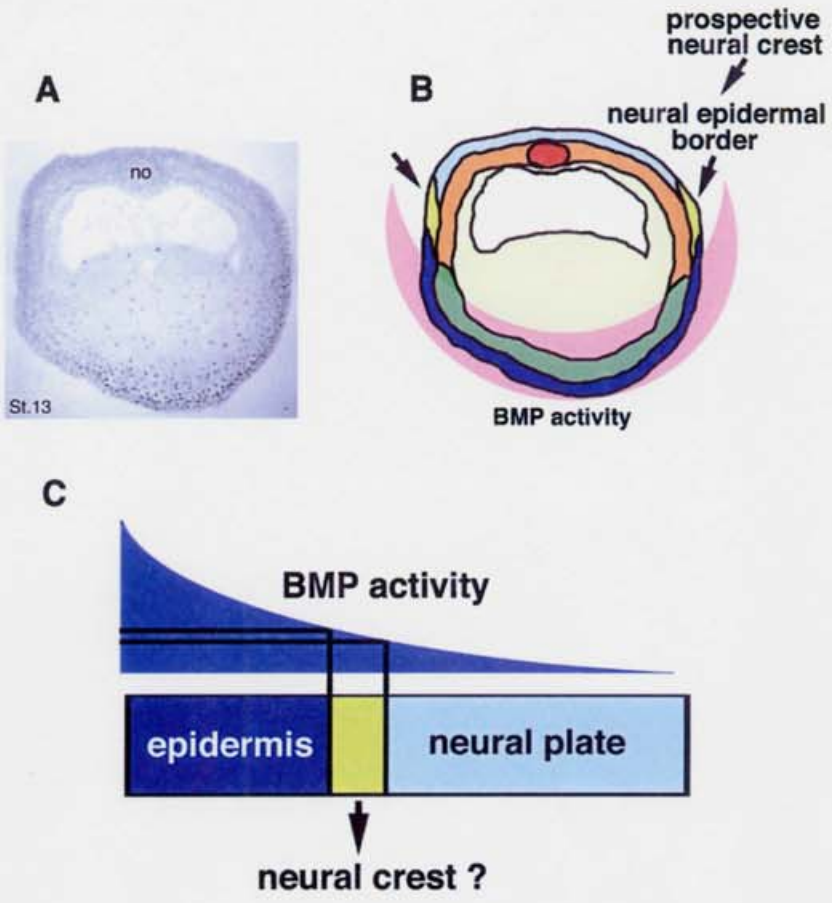

Fig.1-5 PS1 staining pattern in the prospective neural crest region

A: Transverse section of PS1 staining at stage 14. BMP activity was illustrated schematically in **B.**

C: Model of neural crest induction by BMP gradient.

(no, notochord)

BMP activity during the neural tube formation

At stage 14, as the neural fold developed, the signal began to be detectable in the sensorial layer beneath the neural fold (Fig.1-6 A). As organogenesis proceeded, the PS1-positive cells appeared in the dorsal part of the forming neural tube and neural crest cells (Fig.1-6 B). *Msx-1*, one of BMPs target genes, is expressed in this region (Suzuki et al., 1997). At stage 25, PS1 staining was observed at dorsal quarter of the neural tube (Fig.1-6 C). At stage-35 embryo, staining in the dorsal region of the neural tube, which contains the roof plate was observed (Fig.1-6 D). During neural tube forming stages, BMP signaling in dorsal epidermis neighboring neural tube was low. The location of staining in dorsal neural tube also consistent with previous findings showing that BMP family members are dorsalizing factors that have essential functions in specification of dorsal neural tube and the neural crest cells (Lee and Jessell, 1999). On dorsal-ventral patterning of the neural tube *Sonic Hedgehog* (Shh) are reported as long range ventralizing signal. There is strong evidence that the concentration of Shh dictates the position where distinct ventral cell identities arise, developmentally naïve intermediate neural plate explants respond to small incremental changes in the external concentration of Shh protein to give rise to distinct cell fates (Ericson et al., 1997). On my study, distinct gradient of BMP signaling was not observed in the neural tube. So it seems that BMP activity is a short-range signal at least in the dorsal neural tube. As dorsalizing signal, canonical Wnt ligands are also reported (Muroyama et al., 2002). It was demonstrated that absence of Wnt1 and Wnt3a leads to diminished development of most dorsal populations of interneurons (D1 and D2 neurons) and a compensatory increase in D3 neuron populations that neighboring ventrally. BMPs and Wnts may regulate dorsal neural fate cooperatively.

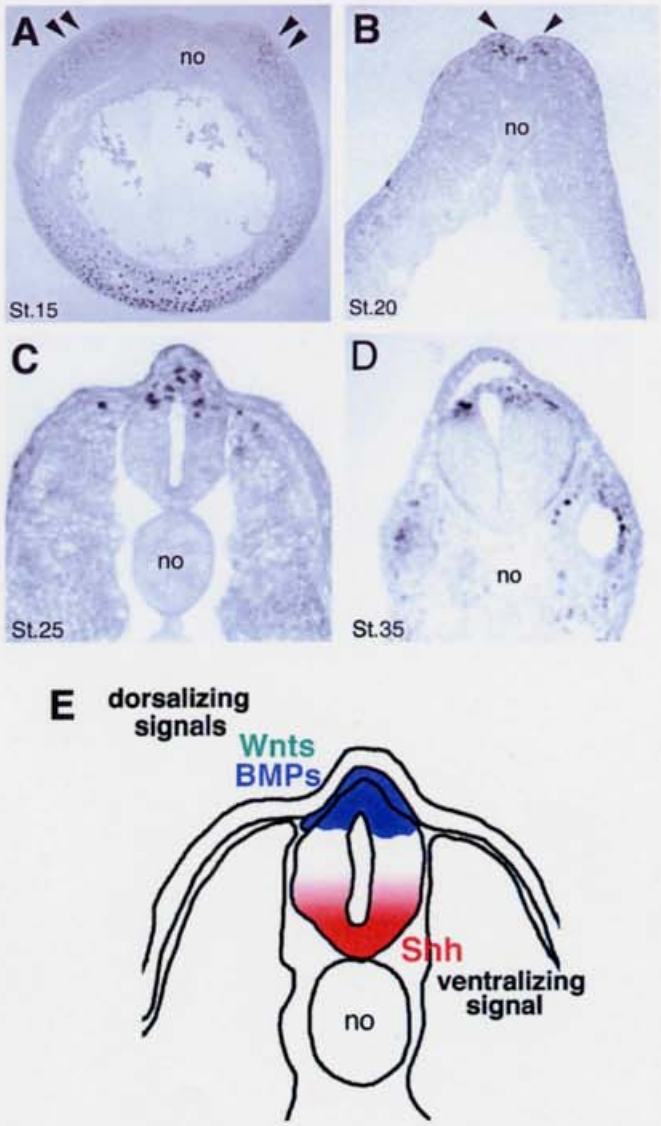

Fig.1-6 PS1 staining pattern during neural tube formation

Xenopus neurula and tail-bad stage embryos were stained with PS1 antibody.

A, B, C, D: Sectioned embryos along D-V axis at stage 15 (**A**), stage 20 (**B**), stage 25 (**C**), stage 35 (**D**). Arrowheads in **A** indicate PS1 positive sensorial layer beneath neural fold. Arrowheads in **G** indicate PS1 positive cells in dorsal part of forming neural tube and neural crest.

(no, notochord)

BMP activity during the eye development

At neurula the PS1 staining was observed in the eye primordia, including the optic vesicle and overlying ectoderm (Fig.1-7 A and D, E). A *BMP7* null mouse displays small eyes with disorganized retinal pigmented epithelium (Dudley et al., 1995; Jena et al., 1997; Luo et al., 1995). BMP4 was also reported to be essential for the interaction between the optic vesicle and the juxtaposing ectoderm (Furuta and Hogan, 1998). My observation of endogenous BMP activity in the developing eye supports the previously proposed role of BMP in eye formation. Consistent with the proposed role of BMP in eye development, strong staining was observed in the dorsal region of the optic vesicle at stage 25 (Fig.1-7 B and F). In chicks, dorsal expression of *BMP4* promotes *Tbx5* expression in the dorsal retina, and the restriction of *Tbx5* to the dorsal neural retina in turn establishes the dorsal identity of the optic nerve in the retinotectal projection (Koshiba-Takeuchi et al., 2000). My observation that BMP activity was confined to the dorsal retina is consistent with the suggested role of BMP4 in the patterning of the retina along the DV axis. At stage-30 and 35 embryos, dorsal parts of the presumptive cornea, pigmented epithelial layer, and anterior lens vesicle showed strong staining (Fig.1-7 C and G, I). This observation provides the first evidence of DV asymmetry in the lens. In the mouse, BMP7 protein is present in the lens placode but exists uniformly along the DV axis (Wawersik et al., 1999). It would be intriguing to find out whether the dorsally localized BMP activity is due to the localized expression of BMP ligands in the dorsal lens or to the influence of BMPs that have emanated from neighboring cells, such as those in the presumptive cornea or pigmented epithelium. It remains to be investigated how BMPs participate in the patterning of the lens, cornea, and pigmented epithelium during eye development.

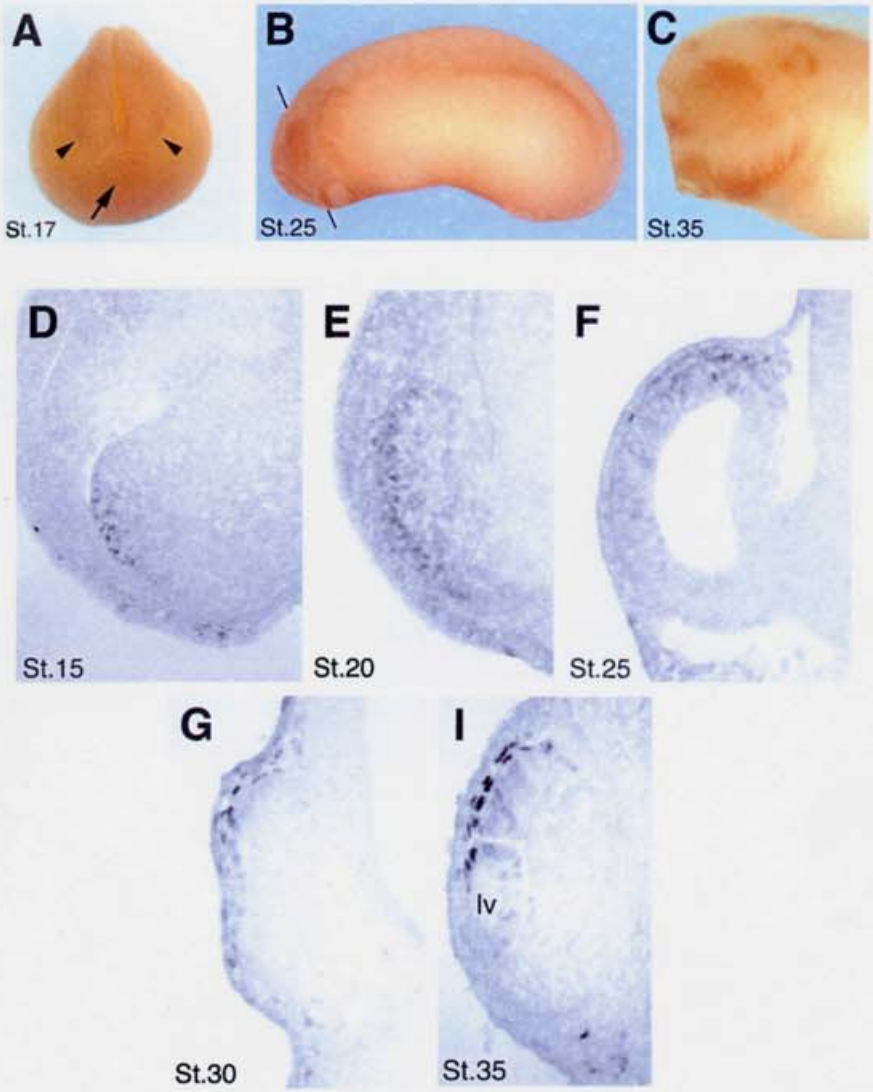

Fig.1-7 PS1 staining pattern during eye development

A, B, C: Whole-mount-stained embryos at stage 17 (**A**), at stage 25 (**B**), at stage 35 (**C**). Arrowheads in **A** indicate staining at the eye primordial and an arrow indicates intensive staining at the presumptive cement gland region. **D, E, F, G, I:** Transverse sections of developing eye at stage 15 (**D**), at stage 20 (**E**), at stage 25 indicated by a line in **B** (**F**), at stage 30 (**G**), at stage 35 (**I**).

In this study, I succeeded in visualizing endogenous BMP signaling during *Xenopus* development using an antibody specific to the activated form of Smads induced by BMP ligands. This type of study, in which endogenous growth factor signals can be visualized, adds profound information that increases my understanding of the signaling and genetic cascade involved in cell differentiation during development.

CHAPTER 2

Xenopus *Nbx*, a novel NK-1 related gene, regulates neural-epidermal border by inhibiting the neural plate fate and direct to neural crest induction

Summary

The vertebrate neural crest is formed at the border between the neural plate and non-neural ectoderm during neurulation and eventually gives rise to a variety of cell types, including neurons, glia, facial chondrocytes and osteoblasts, and melanocytes. Although several secreted molecules such as BMP, Wnts, FGF, and Noelin have been implicated in neural crest formation, little is known about the precise intracellular mechanism underlying neural crest induction. Here, I have identified a novel NK-1 class homeobox gene *Nbx* in *Xenopus* whose expression is correlated with neural crest formation. I also found that *Nbx* harbours an Eh1 domain and is a transcriptional repressor. Overexpression of *Nbx* suppressed neural plate makers, and caused enhanced expression of the neural crest maker *Slug*. Co-injection of dominant-negative form of BMP receptor and *Nbx* caused melanophore induction efficiently in animal caps. In contrast, the overexpression of a dominant-negative form of *Nbx* during neurula stages suppressed the expression of the neural crest marker *Slug* and expanded neural markers such as *Otx2* and *Sox2*. Taken together, I propose that *Nbx* is an essential transcriptional repressor required to permit neural crest induction by inhibiting the neural plate fate.

Introduction

The vertebrate neural crest is formed at the border between the non-neural ectoderm and neural plate during the early stages of neurulation and gives rise to melanocytes, facial cartilage and bone, and neurons and glia of the peripheral nervous system (LeDouarin and Kalcheim, 1999). In *Xenopus*, these cells arise in the neural fold and the dorsal neural tube during neural tube formation and closure. They subsequently migrate ventrally and are distributed to numerous sites and differentiate into various cell types (Mayor and Aybar, 2001). Molecular embryological studies have indicated that several secreted molecules are involved in the cell-cell interactions that induce the neural crest. It has been proposed that an intermediate level of BMP signalling that is generated by the balance between the BMPs and BMP antagonists, such as *Noggin*, *Chordin*, and *Follistatin*, plays a role in establishing the neural crest fate (Barth et al., 1999; Marchant et al., 1998). It was also reported that canonical Wnt signalling enhances neural crest induction, cooperating with BMP antagonists that block BMP signalling (LaBonne and Bronner-Fraser, 1998) and that the inhibition of canonical Wnt signalling suppresses neural crest formation (Garcia-Castro et al., 2002; Ikeya et al., 1997). The blocking of fibroblast growth factor (FGF) signalling using a truncated FGF receptor also suppresses neural crest induction (Mayor et al., 1997). A recent report has shown that a secreted glycoprotein, *Noelin-1*, can induce neural crest cells in the chick (Barembaum et al., 2000). Therefore, it seems that the interplay of several signalling pathways controls the formation of the neural crest. In addition to secreted molecules, several transcription factors that are specifically expressed in the neural crest region have been reported. Zinc finger transcription factor *Zic* genes (Mizuseki et al., 1998; Nakata et al.,

2000; Nakata et al., 1997; Nakata et al., 1998) and winged-helix transcription factor *FoxD3* (Sasai et al., 2001) are not only expressed in the neural crest but also capable of inducing neural crest in the animal cap. The zinc finger transcription factors *Snail* and *Slug* are known to be early markers for the neural crest and are thought to function in the specification and migration of neural crest cells (Carl et al., 1999; LaBonne and Bronner-Fraser, 2000; Mayor et al., 1995). It was also reported that the Sox family transcription factor *Sox9* is required for cranial neural crest development (Spokony et al., 2002). Thus, temporally and spatially regulated functions of these transcription factors appear to be essential for the generation of the variety of cell types and migration of the neural crest.

The NK homeobox genes were first cloned in Drosophila (NK1-NK4) (Kim and Nirenberg, 1989) and encode proteins that can be classified into two homeodomain protein classes, NK-1 (containing NK1) and NK-2 (containing NK2-4), both of which share a conserved Eh1 repressor domain (Smith and Jaynes, 1996). Several NK-related genes have been reported in a variety of animal species. Recently, the functions of NK-2 class homeobox genes have been well characterized by gene disruption experiments in mouse, which have demonstrated that *Nkx-2.5* is an important regulator in heart development (Lyons et al., 1995) and that *Nkx-2.2* is required for ventral specification of the neural tube (McMahon, 2000). In contrast, the functions of the NK-1 class homeobox genes remained to be characterized.

In this study, I have identified a novel NK-1 class homeobox gene, *Nbx*, as an essential component of neural crest induction. *Nbx* expression partially overlapped with the neural crest marker *Slug*. Gain-of-function and loss-of-function analyses have

demonstrated that *Nbx* may be an essential transcription factor to regulate neural-epidermal border by inhibiting the neural plate fate and direct to neural crest induction.

Results

Cloning of the *Nbx* gene

As a part of my effort to identify novel functional genes that regulate early *Xenopus* development, I searched a expression sequence tags (EST) database (XDB: http://xenopus.nibb.ac.jp) for genes encoding homeodomains, and I identified a new gene that contains an NK-1 class homeodomain, which I named *Nbx* (a homeobox gene that expressed in neural-epidermal border). *Nbx* encodes a 255 amino acid protein and includes an Eh1 repressor domain and a homeodomain. The amino acid sequence of Nbx is shown in Fig.2-1A. Its homeodomain has 87% amino acid sequence identity and is most closely related to chick Sax1 (Fig.2-1B). It was previously known that other than the Eh1 motif and homeodomain, there is no obvious conserved sequence among NK-1 class homeobox genes (Duboule, 1994); this turned out to be true for Nbx as well. I performed a homology search against the human, mouse, and zebrafish genome, and the only genes I found that were homologous to Nbx were Sax1 and Sax2, and I was unable to identify apparent orthologs with the same or a very closely related homeodomain sequence to Nbx.

Fig.2-1 *Xenopus Nbx* is a novel NK-1 class homeobox gene

A: Deduced amino acid sequence of the Nbx protein. It has a conserved Eh1 repressor domain (boxed) and a homeodomain (underlined). **B:** Sequence alignment of the Nbx homeodomain with other homeoprotein sequences. Amino acids identical to those of Nbx are indicated by bars, and are expressed as % homology. The sources of the sequences shown are as follows: chick Sax1 (GenBank:P19601), mouse Sax1 (GenBank:P42580), mouse Sax2 (GenBank:AAB53323), *Drosophila* NK1 (GenBank:P22807), *C. elegans* Ceh-1 (GenBank:AAA98004), *Echinococcus* Hbx1 (GenBank:CAA47296), *Drosophila* NK2 (GenBank:B33976), zebrafish Sax1 (gnl|ti|132432270 zfish44766-15a03.q1k in NCBI Zebrafish Traces Archive), zebrafish Sax2 (gnl|ti|31538871 Z35723-a3057g06.p1c in NCBI Zebrafish Traces Archive), human Sax1 (NT_035040.1|Hs10_35202 in NCBI Human Genome), and human Sax2 (NT_006111.12|Hs4_6268 in NCBI Human Genome).

A

```
  1 MGMLDCDPEE EKHAPGQKHL HTP[redacted] NHAKMQKVEE GIKEPDINDE 50
 51 GQTGMTNVRT RMTSESMVSE IENGAGTSPG LQANEPEELP EKEENQQPQN 100
101 LPCATDCKPR RARTAFTYEQ LVALESRFRS SRYLSVCERL SLALTLHLTE 150
151 TQVKIWFQNR RTKWKKQQPT GSWEGRGCSI QNCPTIPGPR INPPLPNYPC 200
201 TTHISHIGAG TNHLSPFPGI FFSPPSTSFG LSPTGATYPQ FIGSSSFTSY 250
251 YSPPL 255
```

B

		identity
Xenopus Nbx	PRRARTAFTYEQLVALESRFRSSRYLSVCERLSLALTLHLTETQVKIWFQNRRTKWKKQQ	
Chick Sax1	----------NK--AT---------N---S-S----------H	87%
Mouse Sax1	----------NK--AT---------N---S-S----------N	87%
Human Sax1	----------NK--AT---------N---S-S----------N	87%
Zebrafish Sax1	----------NK--AT---------N---S-S----------N	87%
Mouse Sax2	----------NK-KAT---------N-G-S-S----------N	83%
Human Sax2	----------NK-KAT---------N---S-S----------N	85%
Zebrafish Sax2	----------NK-K-T---------N---S-S----------N	87%
Dolosophila NK1	----------S--NK-KTT---------N---S-S----------N	83%
Echinococcus EgHbx1	R----------T--NK-Q-T-----Y---N---S-N----------N	80%
C. elegans Ceh-1	M----------NK-KT------V---N--IQ-Q-S----------HN	78%
Drosophila NK2	K-KR-VL--KA-TYE--R---QQ----AP--EH--SLIR--P---------H-Y-T-RA-	55%

Expression of *Nbx* during neurogenesis

As shown in Fig.2-2, the expression of *Nbx* is developmentally regulated. Its mRNA was undetectable before the mid-blastula transition (MBT) by a semi-quantitative reverse transcription-polymerase chain reaction (RT-PCR) analysis. Detectable expression began upon gastrulation at a low level and peaked during neurulation (Fig.2-2 A). The spatial expression pattern was examined by whole-mount *in situ* hybridization and revealed that *Nbx* was predominantly expressed at the border between the neural plate and non-neural ectoderm. At stage 12, four stripes (two per lateral half) of weak staining were observed (Fig.2-2 B). The scattered staining became evident in stage 14 embryos and marked the boundary between the neural plate and non-neural ectoderm (Fig.2-2 C and H). As the neural tube closure proceeded, the striped expression became narrow (Fig.2-2 C-E). From the late neurula stage the anterior component of expression became faint (Fig.2-2 E-F). It is interesting to note that scattered but intense *Nbx* expression was sustained in the posterior trunk, which may reflect an anterior-to-posterior gradient in neural tube maturation. In stage 30 embryos, *Nbx* expression was seen in the region just anterior to the tail bud (Fig.2-2G), and a new expression domain was reproducibly detected as spots in mesencephalon (arrow in Fig.2-2 G and Fig.2-2 I). The expression pattern of *Nbx* was clearly distinct from other previously reported Nk-1 class homeobox genes (Schubert et al., 1995; Spann et al., 1994).

To obtain a more detailed view of the *Nbx* expression pattern, I compared *Nbx* expression to the expression patterns of other regional markers by whole-mount double *in situ* hybridization (Fig.2-2 J-T). *Nbx* was expressed posterior to the anterior neural plate marker *Otx2* (Fig.2-2 J). The outer stripes of *Nbx* were expressed outside the

neural plate markers *Sox2* and *N-CAM*. (Fig.2-2 K, L). The anterior *Nbx* expression of outer stripe coincides with the expression of *Slug*, an early marker for the neural crest (Fig.2-2 M). I could distinguish three expression domains along the AP axis that were, first, the anterior cephalic region expressing only *Slug* (indicated as 1, and corresponding to the mandibular arch in latter stage), second, the posterior cephalic region expressing both *Slug* and *Nbx* (indicated as 2, corresponding to the hyoid and the branchial arches in later stages), and third, the trunk region expressing only *Nbx* (indicated as 3) —trunk expression of *Slug* is induced later. In the overlapping region, the staining for both *Slug* and *Nbx* was in the same ectodermal layer (Fig.2-2 N). The scattered expression of *Nbx* suggested that *Nbx* expression might be regulated by Notch signaling. Thus, I compared *Nbx* expression with the expression of *Delta-1*, which is one of the Notch ligands (Fig.2-2 O). There are few *Delta-1* signals that coincide with the *Nbx* expression of the cranial neural crest region. On the other hand, the inner striped expression of *Nbx* overlapped with the medial stripe of *Delta-1*, which is known to give rise to motor neurons. Because the posterior expression of *Nbx* resembled the expression of *β-tubulin*, which is a known neuronal marker, I compared their expression patterns (Fig.2-2 P-R). *Nbx* expression in the posterior cephalic neural crest region did not coincide with either the medial or intermediate stripes of *β-tubulin* expression. The lateral stripes of *β-tubulin* partially overlapped with the *Nbx* expression, but the outer stripes of *Nbx* expression were wider than the *β-tubulin* stripes were (Fig.2-2 P), as illustrated schematically in Fig.2-2 Q. Finally, an enlarged view demonstrated that the *Nbx*-positive cells in the outer stripe were distinct from *β-tubulin* positive cells (Fig.2-2 R). In later stage embryos, *β-tubulin* was expressed in Rohon-Beard cells and *Nbx* expression became confined to the most dorsal region of the neural

tube (Fig.2-2 S, T).

FIG.2-2 Temporal and spatial expression of *Nbx* during *Xenopus* development

A: Temporal expression patterns of *Nbx*. RNA was extracted from embryos at the indicated stage of development. *Nbx* mRNA expression levels were measured by RT-PCR. The ubiquitous marker *histone H4* served as a control. **B-I:** Spatial expression patterns of *Nbx*. *Nbx* expression was analyzed by whole-mount *in situ* hybridization. (**B**) Stage 12. Black arrowheads in **B** indicate outer stripes and white arrowheads indicate inner stripes of *Nbx* expression. (**C**) Stage 14. (**D**) Stage 18. (**E**) Stage 20. (**F**) Stage 25. (**G**) Stage 30. Arrow in **G** indicates new expression of *Nbx* in mesencephalon, and a transverse section of this region is shown in **I**. (**H**) A transverse section showing the outer stripes at stage 14. (**I**) A transverse section of *Nbx* expressing region in mesencephalon at Stage 30. **J-T:** Comparison between recognized markers and *Nbx* expression. Whole-mount double *in situ* hybridizations were performed with a digoxigenin-labeled *Nbx* probe and a fluorescein-labeled probe for another marker. (**J**) *Nbx* (purple) and *Otx2* (blue) at stage 14. (**K**) *Nbx* (purple) and *Sox2* (blue) at stage 14. (**L**) *Nbx* (purple) and *N-CAM* (blue) at stage 16. (**M, N**) *Nbx* (purple) and *Slug* (blue) at stage16. The 1 in **M** indicates the region where only *Slug* was expressed; the 2 indicates where *Slug* and *Nbx* were coexpressed (a transverse section of this region is shown in **N**); and the 3 indicates where only *Nbx* was expressed. (**O**) *Nbx* (purple) and *Delta-1* (blue) at stage 16. (**P**) *Nbx* (purple) and β-*tubulin* (blue) at stage 16. (**Q**) A schematic representation of the expression of *Nbx* and β-*tubulin*. (**R**) An enlarged view of the outer stripe region at stage16. *Nbx* (purple) and β-*tubulin* (blue). (**S, T**) *Nbx* (purple) and β-*tubulin* at stage 25. The transverse section of posterior region is shown in **T**.

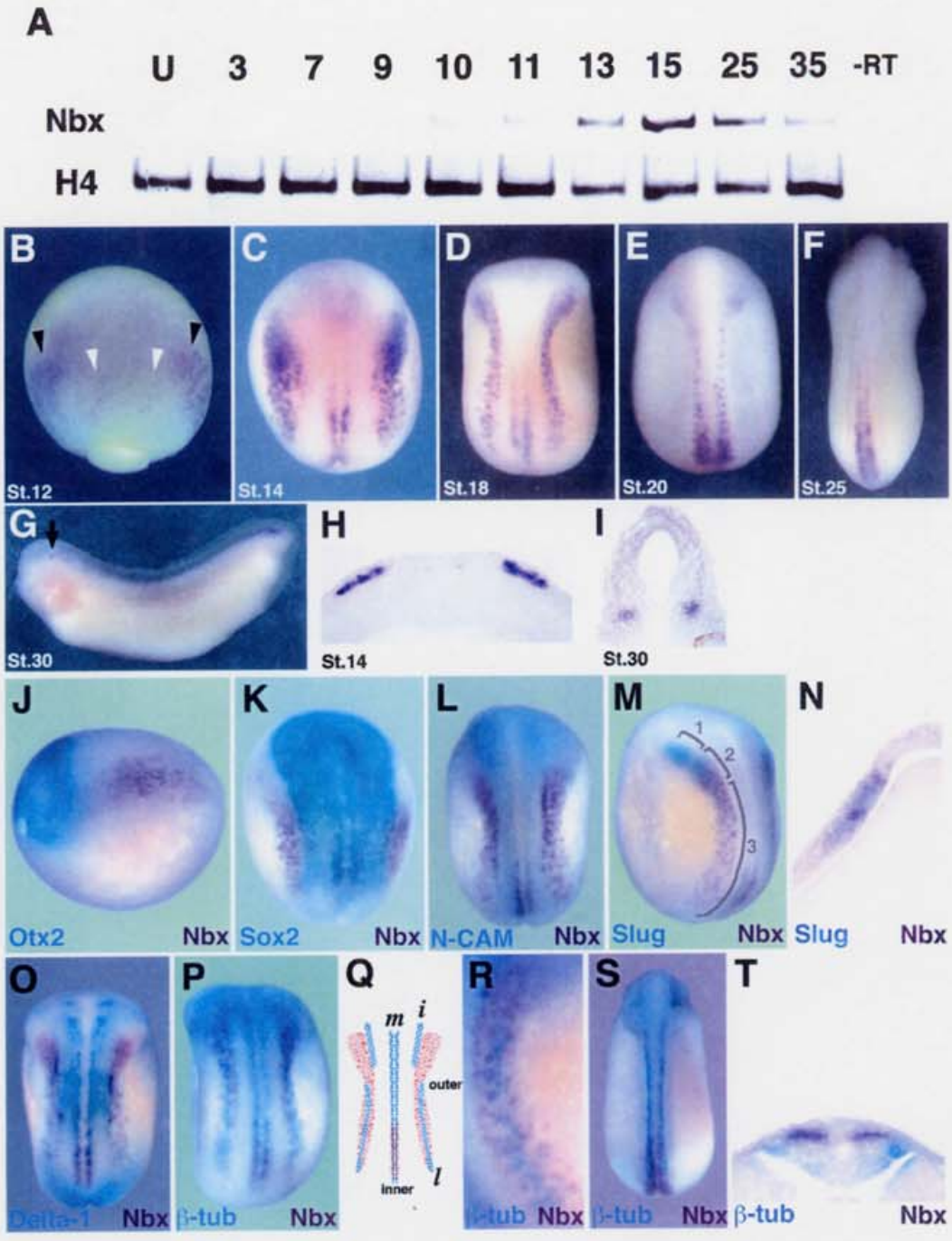
A
U
3
7
9
10
11
13
15
25
35
-RT
Nbx
H4
B
St.12
C
St.14
D
St.18
E
St.20
F
St.25
G
St.30
H
St.14
I
St.30
J
Otx2
Nbx
K
Sox2
Nbx
L
N-CAM
Nbx
M
1
2
3
Slug
Nbx
N
Slug
Nbx
O
Delta-1
Nbx
P
β-tub
Nbx
Q
m
i
outer
inner
l
R
β-tub
Nbx
S
β-tub
Nbx
T
β-tub
Nbx

Nbx expression coincide with neural and neural crest formation

To investigate the regulatory mechanism of *Nbx* gene expression, I examined the expression profile of *Nbx* by whole-mount *in situ* hybridization in embryos in which signaling factors were overexpressed. The overexpression of *BMP4* is known to reduce the neural plate and dorsal mesoderm significantly (Dosch et al., 1997; Wilson et al., 1997), and in such embryos, *Nbx* expression was also reduced (80% n = 10) (Fig.2-3 A). Conversely, the ventral injection of Dominant negative BMP receptor (tBR), which inhibits the endogenous BMP signal, caused a partial (headless) secondary axis, in which the expanded *Nbx* expression was detected between the primary and secondary neural plates (100% n = 10) (Fig.2-3 B). It was previously shown that *neurogenin-related 1* (*Xngnr1*) induces neurons and the neuronal marker *β-tubulin* (100% n =1 0) (Ma et al., 1998) (Fig.2-3 D). Overexpression of *Xngnr1* reduced *Nbx* expression cell-autonomously (90% n = 20) (Fig.2-3 C). This result suggests that *Nbx* is not involved in neurogenin-regulated neuronal induction. *Nbx* expression occurred in a typical salt-and-pepper pattern. Overexpression of *XotchΔE* suppressed not only the expression of *β-tubulin* (85% n = 20) (Fig.3F) but also of *Nbx* (80% n = 20) (Fig.2-3 E). Thus, *Nbx* may be a Notch-regulated gene in *Xenopus*. Overexpression of *Zic3*, which is a known neural and neural crest inducer (Nakata et al., 1997), induced the neural crest marker *Slug* (100% n = 10) (Fig.2-3 H). On the border between the region receiving the *Zic3* injection and the epidermis, I detected the ectopic expression of *Nbx* (90% n = 20) (black arrowheads in Fig.2-3 G). On the anterior border of the *Zic3*-injected region, however, *Nbx* expression was not detected (white arrowhead in Fig.2-3 G). Taken together, these results suggest that *Nbx* expression is induced at the neural-epidermal

border but is restricted to the posterior region of embryo. *Zic5* is also a known neural crest inducer (Nakata et al., 2000). A mutated form of *Zic5* lacking the zinc-finger domain (*Zic5*-ZFC) inhibited neural crest induction (100% n = 10) (Fig.2-3 J) as well as neural induction (100% n = 10) (Fig.2-3 K). *Nbx* expression was also reduced by overexpression of *Zic5*-ZFC (100% n = 20) (Fig.2-3 I).

FIG.2-3 *Nbx* expression coincide with neural and neural crest formation

I injected the mRNAs to several genes into embryos and examined the effect of their forced overexpression on *Nbx* expression by whole-mount *in situ* hybridization.

A: *BMP4* (200 pg) reduced *Nbx* expression. **B:** Overexpression of tBR (500 pg) by injection into the ventral region expanded *Nbx* expression into the induced secondary axis. **C:** *Xngnr1* (100 pg) reduced *Nbx* expression. **D**: *Xngnr1* (100 pg) induced ectopic *b-tubulin* expression. **E-F:** *Xotch*DE (200 pg) injected embryos. (**E**) *Xotch*DE reduced *Nbx* expression. (**F**) *Xotch*DE reduced *b-tubulin* expression. **G:** *Zic3* (200 pg) caused ectopic *Nbx* expression (black arrowheads). The ectopic expression was limited to the posterior region of the injected embryos (white arrowhead). **H:** *Zic3* (200 pg) caused ectopic *Slug* expression. **I:** *Zic5*-ZFC (200 pg) reduced *Nbx* expression. **J:** *Zic5*-ZFC (200pg) reduced *Slug* expression. **K:** *Zic5*-ZFC (200pg) reduced *Sox2* expression.

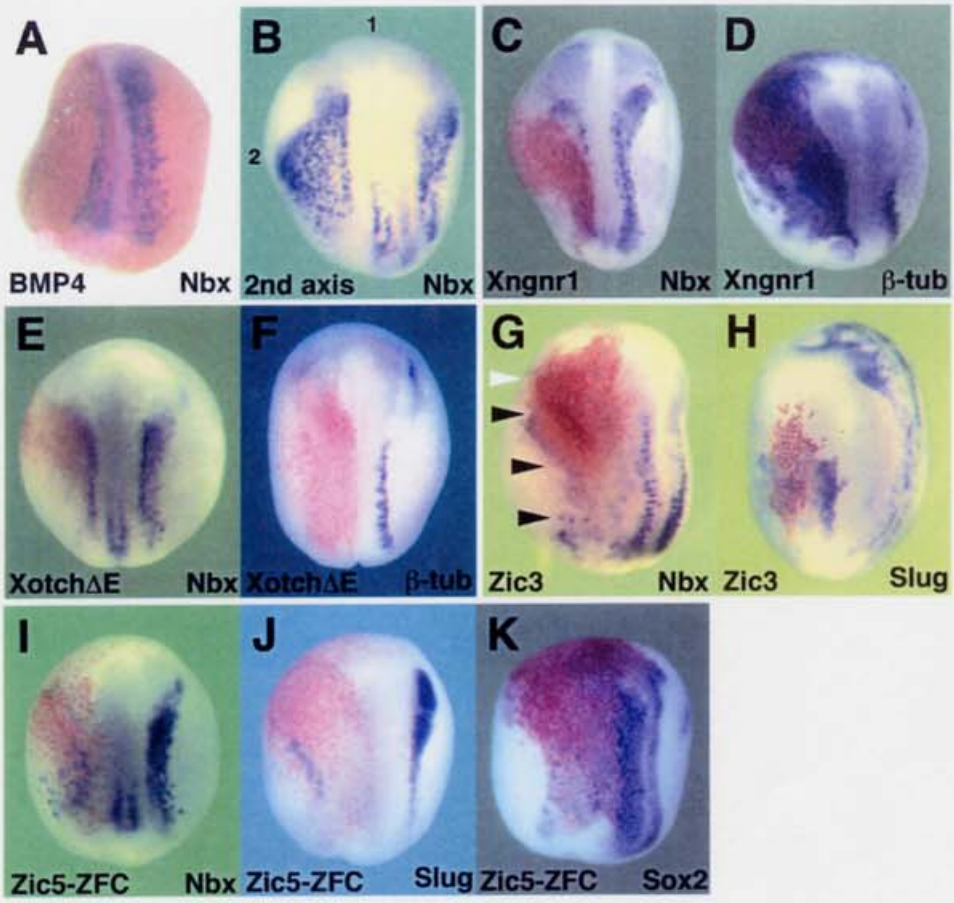
A
BMP4
Nbx
B
1
2
2nd axis
Nbx
C
Xngnr1
Nbx
D
Xngnr1
β-tub
E
XotchΔE
Nbx
F
XotchΔE
β-tub
G
Zic3
Nbx
H
Zic3
Slug
I
Zic5-ZFC
Nbx
J
Zic5-ZFC
Slug
K
Zic5-ZFC
Sox2

Overexpression of *Nbx* suppressed the Spemann organizer

To understand the possible function of *Nbx*, a gain-of-function analysis was performed by injecting its mRNA. Embryos that received an injection of 200 pg of *Nbx* mRNA in the dorsal side at the 4-cell stage displayed a head defect (93% n = 30) (Fig.2-4 B, C). Analysis by *in situ* hybridization at gastrula stage showed that the organizer markers *Otx2* and *goosecoid* were down-regulated cell-autonomously by the overexpression of *Nbx* with β-gal as a linage tracer (*Otx2*, 100% n = 20; *goosecoid*, 90% n = 20) (Fig.2-4 D, E).

Nbx act as a transcriptional suppressor

Because Nb*x* has an Eh1 repressor motif, I expected that Nbx would have a transcriptional repressor activity. To examine this possibility, I fused Nbx to previously characterized activating or repressing domains: the activator domain of VP16 (VP) and the repressor domain from Drosophila engrailed (EnR). A schematic representation of these constructs is shown in Fig.2-4 A. The injection of VP-*Nbx* mRNAs (50 pg) into the dorsal side of 4-cell stage embryos caused a defect in gastrulation movement (data not shown). In contrast, overexpression of VP-*Nbx* (50 pg) in the ventral side caused ectopic cement-gland induction (87% n = 30) (black arrowhead in Fig.2-4 L, compare with M). These phenotypes are very similar to the overexpression phenotypes of *Otx2* (Blitz and Cho, 1995). *In situ* hybridization analysis showed that the overexpression of VP-*Nbx* in dorsal side expanded *Otx2* (100% n = 10) and *goosecoid* (100% n = 10) expression (Fig.2-4 N, O). *Nbx* overexpression in the ventral side caused ectopic expression of *Otx2* (100% n = 10) and *goosecoid* (100% n = 10) (Fig.2-4 P, Q).

Injection of EnR-*Nbx* mRNAs (50 pg) into the dorsal side reduced the expression of organizer markers (data not shown) and caused a defect in head formation (83% n = 30) (Fig.2-4 N, O). From these data, I conclude that VP-Nb*x* has the opposite activity to native Nbx, and EnR-Nbx's activities are indistinguishable from native Nbx. Therefore, I have tentatively concluded that Nbx acts as a transcriptional suppressor *in vivo*.

FIG.2-4 *Nbx* acts as a transcriptional suppressor

A: Schematic representation of *Nbx*, VP-*Nbx*, and EnR-*Nbx* constructs. **B:** Phenotypes of *Nbx* (200 pg)-injected embryos. The *Nbx* injection into the dorsal side caused a head defect. **C:** Uninjected embryos developed normally. **D, E:** Whole-mount *in situ* hybridization analysis of *Nbx* (200 pg)- and b-gal (100 pg)-injected embryos at stage 11. *Nbx* suppressed the organizer markers *Otx2* (**D**) and *goosecoid* (**E**). **F, G:** Whole-mount *in situ* hybridization analysis of b-gal (100 pg)-injected embryos. β-gal injection did not affect the expression of *Otx2* (**F**), *goosecoid* (**G**). H: Phenotype of VP-*Nbx* (100 pg)-injected embryo. The VP-*Nbx* injection into the ventral side caused ectopic cement gland formation (arrowhead in **H**). **I:** Uninjected embryos developed normally. **J-M:** Whole-mount *in situ* hybridization analysis of VP-*Nbx* (100 pg)- and b-gal (100 pg)-injected embryos. VP-*Nbx* injection into the dorsal side led to the expanded expression of *Otx2* (**J**) and *goosecoid* (**K**). VP-*Nbx* injection into the ventral side resulted in the ectopic expression of *Otx2* (**L**) and *goosecoid* (**M**) at the injected region. **N:** Phenotype of EnR-*Nbx* (100 pg)-injected embryo. The injection caused a head defect. **O:** Uninjected embryos developed normally.

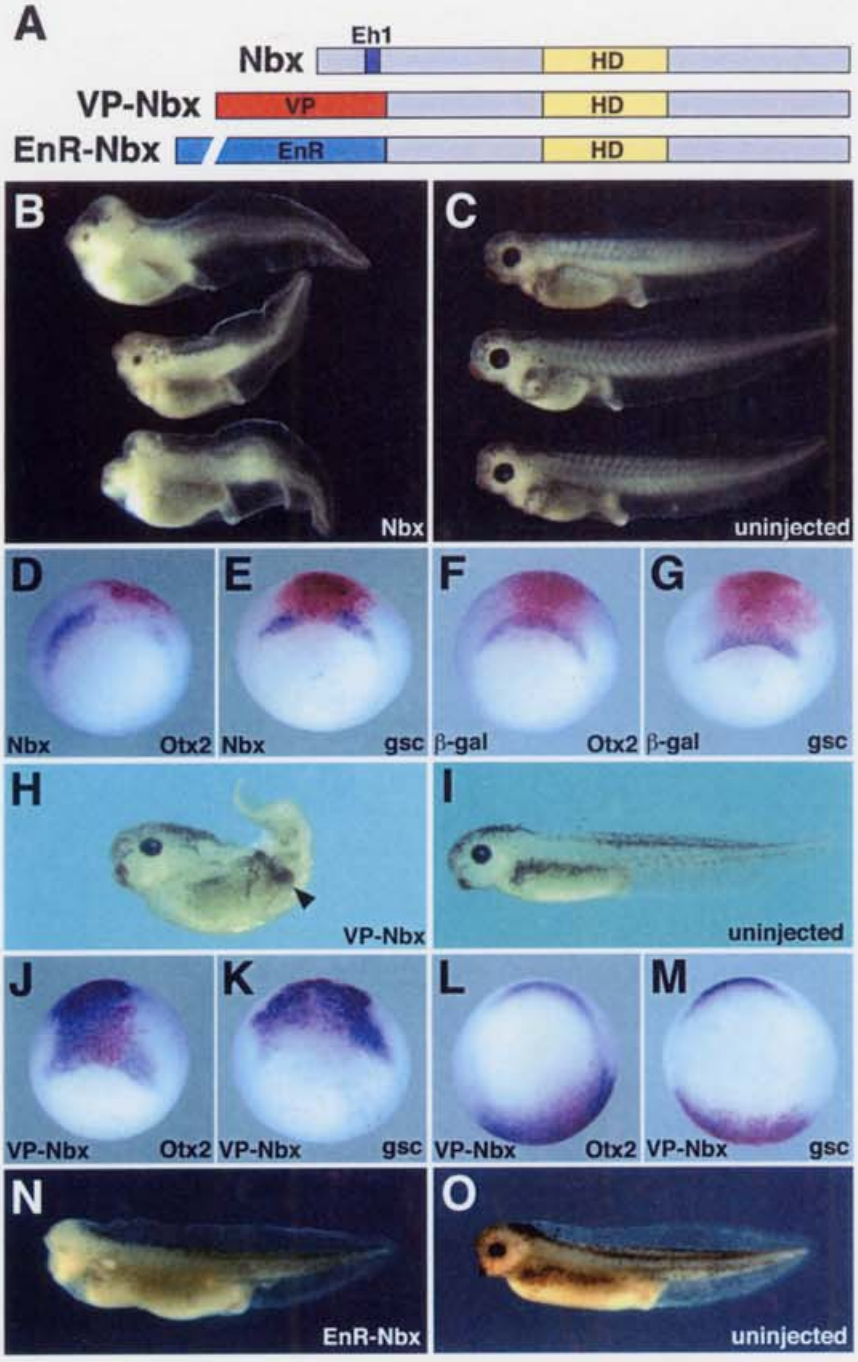
A
Eh1
Nbx
HD
VP-Nbx
VP
HD
EnR-Nbx
EnR
HD
B
Nbx
C
uninjected
D
Nbx
Otx2
E
Nbx
gsc
F
β-gal
Otx2
G
β-gal
gsc
H
VP-Nbx
I
uninjected
J
VP-Nbx
Otx2
K
VP-Nbx
gsc
L
VP-Nbx
Otx2
M
VP-Nbx
gsc
N
EnR-Nbx
O
uninjected

Overexpression of *Nbx* at lateral neural region suppressed neural plate makers and caused enhanced neural crest formation

Because early overexpression of *Nbx* at dorsal marginal zone suppressed the organizer genes and it was difficult to understand its role in later embryogenesis, I attempted to target overexpression of *Nbx* in prospective lateral neural region by injecting *Nbx* mRNA into a lateral animal blastomere of 16-cell stage embryo (Wallingford and Harland, 2002). Injection of *Nbx* mRNA (100pg) and β-gal mRNA (100pg) into a lateral animal blastomere of 16-cell stage embryo fated to neural and neural-epidermal border suppressed anterior neural plate maker *Otx2* (Fig.2-5 B) and pan-neural plate makers *N-CAM* and *Sox2* (Fig.2-5 C, D). In contrast, the expression of *epidermal keratin* was expanded into the neural plate (Fig.2-5 E). Neural crest maker *Slug* was initially suppressed at early neurula (Fig.2-5 F), but at later stages, enhanced *Slug* expression was observed at injected region (Fig.2-5 G, H, I).

Next, I examined *Nbx* activities in neuralized animal caps in the absence of mesoderm. Dominant negative form of BMP receptor (tBR) mRNA (300pg) was injected alone or co-injected with *Nbx* mRNA (100pg) into the animal pole of 2-cell stage embryos. Animal caps were excised at stage 8.5 and cultured until sibling embryos developed to late neurula stage (stage 20). The expression of molecular markers in the animal caps was analyzed by RT-PCR. Overexpression of tBR in animal caps induced anterior neural maker *Otx2* in the absence of mesoderm (lane 1 in Fig.2-5 J). When tBR and *Nbx* were co-expressed in animal caps, the expression of *Otx2* was suppressed, and instead *Slug* was induced (lane 2 in Fig2-5. J). After 2 days incubation (stage 40), tBR and *Nbx*

co-injected animal caps (85% n = 40) accumulated a significant number of melanophores (Fig.2-5 K), in contrast to uninjected (0% n = 40) or tBR injected (0% n = 40) caps. In only *Nbx* injected animal caps, these makers were not affected at stage 20 by RT-PCR analysis (lane 6 in Fig.2-5 J) and melanophores were not observed at stage 40 (data not shown).

FIG.2-5 Overexpression of *Nbx* in lateral neural plate suppressed neural plate makers and caused enhanced neural crest formation

A: Schematic representation of the *Nbx* construct. **B-I:** Whole-mount *in situ* hybridization analysis of *Nbx*-injected embryos. Each panel shows two embryos with the same treatment. (**B-D**) Expression of neural plate makers. Overexpression of *Nbx* suppressed neural plate makers *Otx2* (**B**), *N-CAM* (**C**) and *Sox2* (**D**). (**E**) Overexpression of *Nbx* expanded the expression of *epidermal keratin* into the neural plate. (**F-I**) Expression of neural crest maker *Slug*. *Slug* was reduced at stage 15 (**F**), but enhanced *Slug* expression was observed at injected region at stage 20 (**G, I**) and stage 25 (**H**). **J:** RT-PCR analysis of gene expression in the animal caps at stage 20 equivalent that were injected with 300pg tBR mRNA (lane 1), co-injected with 300pg tBR and 100pg *Nbx* mRNA (lane 2), uninjected (lane 3), and njected with 100pg *Nbx* mRNA alone (lane 6). The expression of makers in sibling whole embryo (lane 4). The control reactions with no reverse transcription step (lane 5, 7). **K:** Animal caps co-injected with 300pg tBR and 100pg *Nbx* contained melanophores at stage 40 equivalent (Black spots in **K**). (Blown pigments were not melanophores, they were pigment granules derived from the egg.) **L:** Uninjected animal caps at stage 40 equivalent.

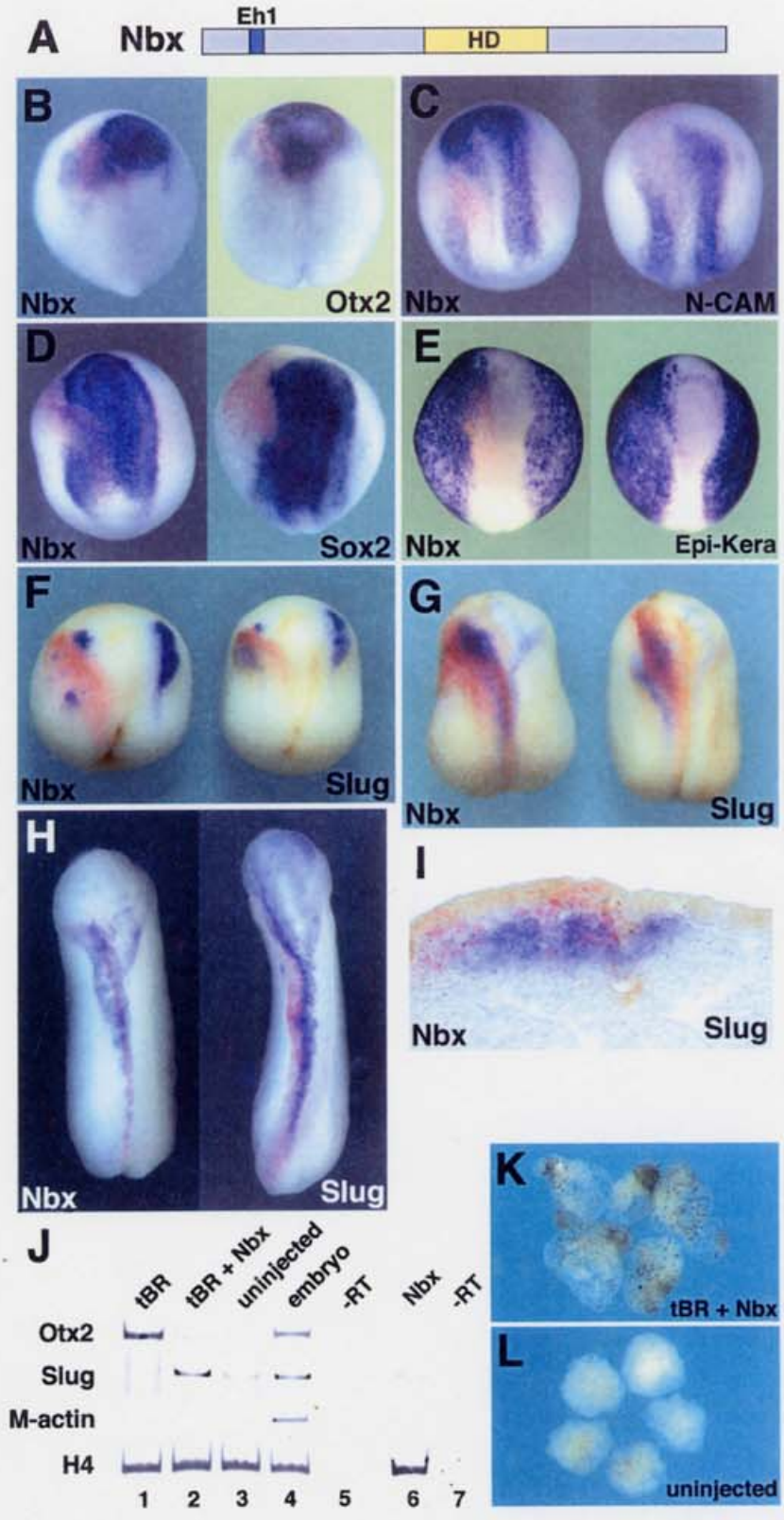
A
Nbx
Eh1
HD
B
Nbx
Otx2
C
Nbx
N-CAM
D
Nbx
Sox2
E
Nbx
Epi-Kera
F
Nbx
Slug
G
Nbx
Slug
H
Nbx
Slug
I
Nbx
Slug
J
tBR
tBR + Nbx
uninjected embryo
-RT
Nbx
-RT
Otx2
Slug
M-actin
H4
1 2 3 4 5 6 7
K
tBR + Nbx
L
uninjected

Overexpression of VP-*Nbx*-GR with DEX addition from Stage 13 caused neural plate expansion and suppressed the neural crest

To clarify the endogenous role of Nbx, I attempted a knock-down of *Nbx* function *in vivo* using morpholino antisense oligonucleotides (sequence: ACATTCCCATGTAGCTCCAGATAGT). However, 8 nl of 0.2 mM *Nbx* morpholino oligo injection caused abnormal gastrulation cell movements. As I failed to rescue the phenotypes by injecting wild-type *Nbx* mRNA, it seemed that these phenotypes were not gene-specific effects, but were similar to the artificial effects of morpholino oligos that have been reported previously (Heasman, 2002). Therefore, I tried another experiment to inhibit endogenous *Nbx* functions. Previous studies have shown that conversion of a transcriptional repressor to an activator, or the converse, can generate a dominant form that antagonizes the endogenous protein (Yamamoto et al., 2001). In fact, VP-*Nbx* caused an opposite effect to native *Nbx* (Fig.2-3).

Because early overexpression of VP-*Nbx* during the blastula and gastrula stages induced the organizer genes in the injected region, I was unable to elucidate the in vivo role of *Nbx* during the neurula stage. Therefore, I attempted to overexpress VP-*Nbx* later in embryogenesis in a temporally controlled manner without affecting the organizer formation, through the conditional expression of VP-*Nbx* in a hormone-inducible form, that is, as a fusion protein with the glucocorticoid receptor (GR) (Kolm and Sive, 1995). The function of endogenous *Nbx* at the neurula stage was examined by fusing the VP16 activator domain and the GR domain to the *Nbx* homeodomain (VP-*Nbx*-GR; Fig.2-6 A).

Injecting VP-*Nbx*-GR mRNA (100 pg) and β-gal mRNA (100 pg) into the dorsal side with the addition of DEX from the 8-cell stage caused the expansion of organizer marker expression; this was also seen in embryos injected with VP-*Nbx* mRNA and these effects were rescued by co-injection of native *Nbx* (data not shown). Thus, it seems that VP-*Nbx* and VP-*Nbx*-GR with early DEX addition had similar functions. Importantly, the injection of VP-*Nbx*-GR (100 pg) and β-gal (100 pg) into the left side with DEX addition from stage 13 reduced the expression of the neural crest marker *Slug* and expanded the expression of neural plate markers (*Sox2* and *Otx2*) cell-autonomously in the injected region (100% n = 20 each) (Fig.2-6 B, D, F). *Epidermal keratin* was also reduced on the injected side (100% n = 10) (Fig.2-6 H). It is evident that these effects required DEX addition, because the expression of the marker genes was normal in the absence of DEX (Fig.2-6 C, E, G, I). Co-injection with *Nbx* (200pg) rescued the neural plate expansion by VP-*Nbx*-GR with DEX addition from stage 13 (90% n = 20) (Fig.2-6 J). These results suggest that *Nbx* contributes to neural crest differentiation at the expense of neural plate fate and are consistent with the results of wild type *Nbx* overexpression that lead to the repression of neural plate fate.

FIG.2-6 Overexpression of VP-*Nbx*-GR with DEX addition from stage 13 suppressed neural crest induction and expanded neural plate markers

A: Schematic representation of the VP-*Nbx*-GR construct. **B-I:** Whole-mount *in situ* hybridization analysis of VP-*Nbx*-GR-injected embryos with DEX addition from stage 13 (**B, D, F, H**) and without DEX addition (**C, E, G, I**). Each panel shows two embryos with the same treatment. (**B**) Overexpression of VP-*Nbx*-GR with DEX addition from stage 13 suppressed induction of neural crest maker *Slug*. (**C**) The VP-*Nbx*-GR injection without DEX addition did not affect *Slug* induction. (**D, F, H**) Overexpression of VP-*Nbx*-GR with DEX addition from stage 13 expanded the expression of the neural plate marker *Sox2* (**D**) and the anterior neural plate marker *Otx2* (**F**) at the injected region and suppressed the epidermal marker *epidermal keratin* (**H**). (**E, G, I**) The VP-*Nbx*-GR injection without DEX addition did not affect *Sox2* (**E**), *Otx2* (**G**), or *epidermal keratin* (**I**). **J:** Co-injection of VP-*Nbx*-GR (100pg) and *Nbx* (200pg) and β-gal (100 pg) with DEX addition from stage 13. *Nbx* rescued *Sox2* expansion by VP-*Nbx*-GR.

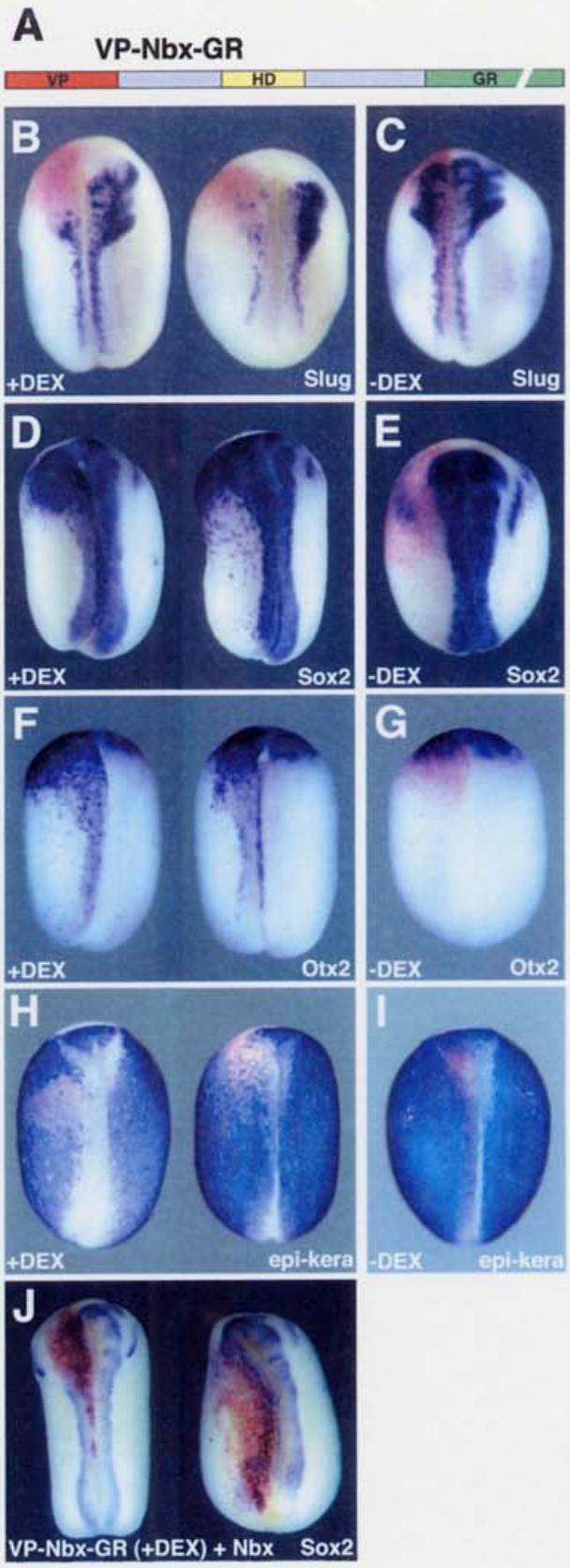
A
VP-Nbx-GR
VP
HD
GR
B
+DEX
Slug
C
-DEX
Slug
D
+DEX
Sox2
E
-DEX
Sox2
F
+DEX
Otx2
G
-DEX
Otx2
H
+DEX
epi-kera
I
-DEX
epi-kera
J
VP-Nbx-GR (+DEX) + Nbx
Sox2

Discussion

Regulation of *Nbx* expression

In this study, I isolated and characterized a novel homeobox gene, *Nbx*, which was expressed at the neural-nonneural border of the *Xenopus* neurula. Like other NK-1 class homeobox genes, Nbx has a conserved Eh1 repressor domain at the N-terminal region and acts as a transcriptional repressor as described. Comparing the expression pattern of *Nbx* to the expression of several molecular markers, I noted that *Nbx* expression partially but significantly overlaps with neural crest markers. *Nbx* expression was also found to be activated by neural and neural crest inducers. Both the endogenous and ectopic *Nbx* expression was restricted to the posterior part of the embryos, suggesting that *Nbx* induction depends on endogenous posteriorizing signals (e.g., Wnts, FGFs). Known neural crest markers are first induced in the cranial region and later expand into the trunk region (Mayor et al., 1995; Sasai et al., 2001; Spokony et al., 2002). In contrast, *Nbx* expression is induced throughout the AP axis with the same timing, although the expression becomes faint in the anterior region in later stages. Expression of *Nbx* is a typical "salt and pepper" pattern, may be regurated by *Notch* signaling, but there are few *Delta1* expressing cells in the cranial neural crest region in *Xenopus* (Fig.2-2 O). Therefore, it is possible that other *Notch* ligands (e.g., Serrate-1) regulate *Nbx* expression in this anterior region.

Functions of *Nbx* in neural crest development

The overexpression of *Nbx* suppressed and of VP-*Nbx* expanded the expression of organizer markers. However, the level of the *Nbx* mRNAs during the organizer-forming stages, as revealed by RT-PCR analysis, was rather low, and I was unable to detect specific signals by whole-mount *in situ* hybridization at these stages. Therefore, it is unlikely that *Nbx* regulates organizer formation *in vivo*. Rather, I propose that *Nbx* is an essential component of the system that regulates neural crest formation,. The gain-of-function analysis showed that *Nbx* suppressed neural plate makers. The inhibition of neural induction by *Nbx* overexpression during neurogenesis caused expansion of epidermal maker into the neural plate, and suppressed neural crest induction at early neurula. In later stages, however, enhanced *Slug* expression at the injected region. The downreguration of neuralized level by *Nbx* overexpression may be a part of a cause of the neural crest induction as demonstrated in Fig.2-5 J. It may be presumed that overexpression of *Nbx* in the neural plate caused ectopic neural-epidermal border providing a condtion suitable for neural crest induction. *Nbx* is not likely to be a direct neural crest inducer because *Nbx* could not induce *Slug* expression alone in the animal caps. Interestingly, co-injection of tBR and *Nbx* caused melanophore induction efficiently in animal caps. It seems that *Nbx* promoted neural crest induction positively in this condition. Overexpression of a dominant-negative form of *Nbx* (VP-*Nbx*-GR) expanded the neural plate markers and suppressed neural crest marker. Many neural crest inducers are known to induce neural plate markers as well (Nakata et al., 2000; Nakata et al., 1997; Nakata et al., 1998; Sasai et al., 2001). However, in *Xenopus*, the neural crest is formed in a region that is distinct from the neural plate. Therefore, I

speculate that *Nbx* may be an essential transcription factor to regulate neural-epidermal border by inhibiting the neural plate fate, which is essential for neural crest formation.

CONCLUSIONS

The pattern of BMP signaling visualized in this work supports the model of neural and epidermal induction by BMP activity. Furthermore, I have demonstrated that a novel homeobox gene *Nbx* may be essential for rigorous regional specification on neural-epidermal border and neural crest induction in the downstream process of pattern formation by BMP activity.

I show a model of ectodermal patterning in Fig.3 as a conclusion of this study.

Ectoderm is initially differentiated into ventral ectoderm and dorsal ectoderm. Ventral ectoderm is leaded by zygotic expression of BMPs, and dorsal ectoderm is leaded by inhibition of BMP signaling by BMP antagonists secreted form Spemann's organizer. On dorsal ectoderm several neuralizing factors that are able to induce both neural crest makers and neural plate makers, such as *Zic*-related genes (Mizuseki et al., 1998; Nakata et al., 2000; Nakata et al., 1997; Nakata et al., 1998) are induced. *Zic* genes initially expressed at entire dorsal ectoderm, at later their expression is restricted to lateral region of the dorsal ectoderm. It was reported that *Zic1* is suppressed by Shh signals in center of dorsal ectoderm (Rohr et al., 1999). *Nbx* is induced at the border between prospective neural plate and prospective epidermis on downstream of Zic-related genes. *Nbx* expression seems to be also regulated by Notch signaling. *Nbx* suppress the neural plate fate and enhanced neural crest fate. Thus neural crest is formed at the neural-epidermal border.

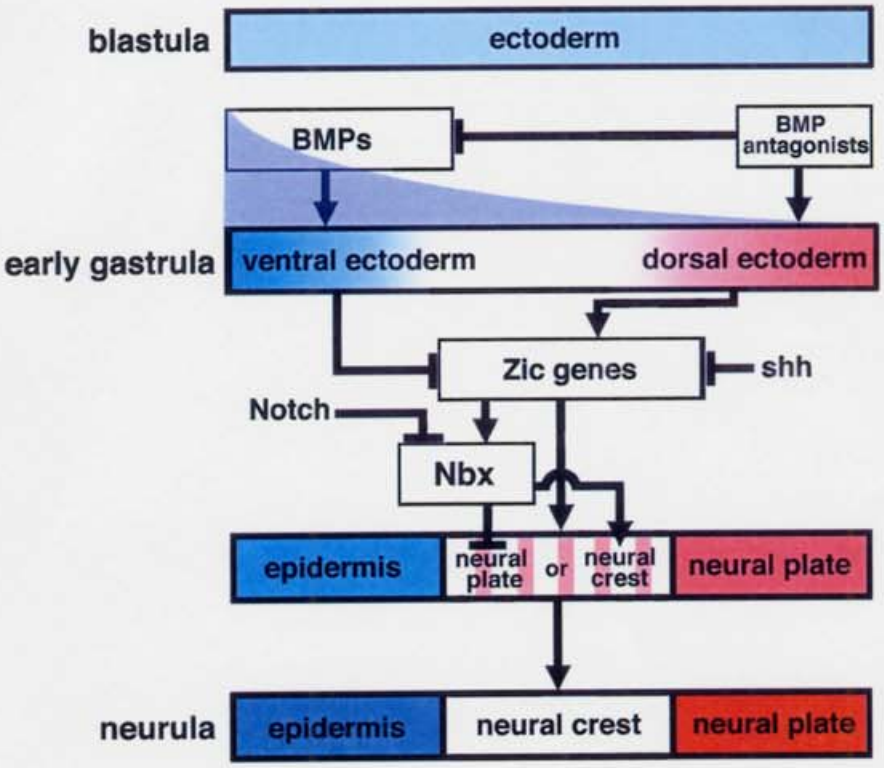

FIG. 3 Model of neural crest induction

MATERIALS AND METHODS

Manipulation of embryos and microinjection of mRNA

Unfertilized eggs were collected and fertilized in vitro as described previously (Suzuki et al., 1994). mRNAs were injected into 2-cell or 4-cell or 8-cell or 16-cell stage embryos. The embryos were cultured in 3% Ficoll/0.1x Steinberg's solution until the appropriate stage for each experiment. They were staged according to Nieuwkoop and Faber (Nieuwkoop, 1967). For animal cap assay, animal caps were dissected at stage 8.5 and cultured in 0.1% BSA/1x Steinberg's solution (Asashima et al., 1990)

Antibody

PS1 antibody was gifted from Dr. Peter ten Djike.

Immunohistochemistry

Embryos were fixed in MEMFA (0.1 M MOPS pH 7.4, 2 mM EGTA, 1 mM $MgSO_4$, 3.7% formaldehyde) for 1 hour, rinsed with PBS (phosphate buffered saline) three times, and stored in 100% methanol at –20 °C. They were bleached in 10% H_2O_2 in methanol for 3 hours under bright light. The embryos were then washed in PBSTw (0.1% Tween-20 in PBS), blocked with FCS-PBS (15% Fetal calf serum in PBS) for 20 min and incubated overnight at 4 °C with the first antibody (1:500) in FCS-PBS. They were washed with PBSTw, blocked with FCS-PBS, and incubated for 2 hours at room temperature with HRP-conjugated goat anti-rabbit IgG (1:500). The embryos were then washed with PBSTw, and incubated with 0.05% DAB solution for 30 min. Staining was

developed by adding H_2O_2. Stained embryos were re-fixed in MEMFA and embedded in acrylamide solution, which was then polymerized. The polymerized block was sectioned at 10-20 mm with a cryostat (Reichert-Jung 2800 Frigocut Cryostat).

Clearing the embryos

Re-fixed, stained embryos were rinsed with 100% methanol three times and incubated with 100% Benxyl Benzoate.

Western blot analysis

Ten pieces of animal cap were isolated at stage 8.5 and homogenized in 20µl of lysis buffer (150 mM NaCl, 50 mM Tris pH 8.0, 1% Triton X-100, 2 mM EDTA, 20 µg /ml aprotinin, 40 µl/ml leupeptin, 4 µg/ml pepstatin, 0.75 mM PMSF, 25 mM b-glycerophosphate, 1 mM Na_3VO_4, 100 mM NaF). The lysates were centrifuged at 14000 rpm for 15 minutes in tabletop centrifuge at 4 °C, suspended in twice their volume of 2 X laemmli buffer and boiled. They were separated by 7.5 % SDS-polyacrylamide gel electrophoresis (SDS-PAGE) and transferred to PVDF membrane (BioRad). The membrane was blocked overnight at room temperature (RT) with 5% skim milk in Tris-buffered saline plus Tween 20 (10mM Tris pH 8.0, 150mM NaCl, 0.2% Tween 20), and then incubated overnight with the primary antibody. After washing in the Tris-bufferd saline plus Tween 20, the membrane was incubated with HRP-conjugated secondary antibody for 2 hours at RT, and washed and developed with chemiluminescent regents (Amersham).

Isolation of Nbx

I searched for new genes containing homeodomains in an EST database (http://xenopus.nibb.ac.jp) using the BLAST search protocol. We examined the expression pattern of several clones by whole-mount *in situ* hybridization and decided to focus on clone XL90n01 (*Nbx*-pBS SK-). GenBank sccession number is BJ092031.

Plasmid construction

The entire coding region of *Nbx* was subcloned into the pCS2 vector (*Nbx*-pCS2). To generate the VP-*Nbx* and EnR-*Nbx* constructs, Nbx lacking the Eh1 repressor domain (amino acids 34-255) was subcloned into the VP16-pCS2 or EnR-pCS2. VP16-pCS2 was a gift from Dr. K.W. Cho. Drosophila engrailed cDNA in pBS was a gift from Dr. J. C. Corbo, and its repressor domain (amino acids 1-298) was subcloned into pCS2. To generate the GR fusion constructs, the human glucocorticoid receptor ligand-binding domain from the *Bra*-GR construct (Tada et al., 1997) was subcloned into pCS2. The coding region of VP-*Nbx* was amplified by PCR and subcloned into GR-pCS2. *Zic3*-pCS2-MT (Nakata et al., 1997) and *Zic5*-ZFC-pCS2-MT (Nakata et al., 2000) were gifted from Dr. J. Aruga. *Xotch*ΔE-pCS2 (Coffman et al., 1993), *Xngnr1*-pCS2-MT (Ma et al., 1998) and DN-BMPR-pSP64T (Suzuki et al., 1995) were also used. For mRNA injection, the plasmids were linearized with Asp718 (EnR-*Nbx*), EcoRI (DN-BMPR) or NotI (the other constructs), and transcribed using the mMESSAGE mMACHINE Sp6 kit (Ambion), then purified by passing them through a Sephadex G-50 column (Amersham Pharmacia Biotech).

Reverse transcription-polymerase chain reaction (RT-PCR)

Total RNA was extracted from the embryos using TRIzol reagent (GIBCO/BRL). Extracted RNA was subjected to reverse transcription with random hexameric primers. The expression levels of maker genes were detected by PCR using the following specific primers.

Nbx (F: 5'-GCAGACATACTGAACCATGC-3', R: 5'-AAGGGCCACAAGCTGCTCGT-3'; 22 cycles)

Slug (F: 5'-ATGCACATCAGGACACACAC-3', R: 5'-CAGCAACCAGATTCCTCATG-3'; 20 cycles)

Muscle actin (F: 5'-TCCCTGTACGCTTCTGGTCGTA-3', R: 5'-TCTCAAAGTCCAAAGCCACATA-3'; 16 cycles)

Otx2 (F: 5'-GGAGGCCAAAACAAAGTG-3', R: 5'-TCATGGGGTAGGACCTCT-3'; 18 cycles)

The primer sequence of *Histone H4*, an internal input control, was as previously described (Iemura et al., 1998).

Lineage tracing and whole-mount in situ hybridization

Embryos receiving coinjections of the mRNA of each construct and β-galactosidase mRNA were fixed in MEMFA ((0.1 M Mops (pH 7.4), 2 mM EGTA, 1 mM MgSO4, 3.7% formaldehyde)), washed with PBS, and stained with 6-chloro-3-indolyl-b-D-galactoside for lineage labeling (red; Nacalai tesque). Stained embryos were then

refixed in MEMFA and stored in methanol at -30°C. Whole-mount *in situ* hybridization was performed as described previously (Suzuki et al., 1997). For double *in situ* hybridization, one fluorescein-labeled probe was stained with BCIP (light blue; Roche) and the other DIG-labeled probe was stained BM purple (Indigo; Roche). Template plasmids for probe synthesis were as follows: *β-tubulin* in pGEM3Zf (a gift from Dr. H. Takabatake), *Delta-1* in pT7Blue (a gift from Dr. M. Mochii), *Otx2* in pBS (Blitz and Cho, 1995), *Slug* in pMX363 (Mayor et al., 1995), *N-CAM* in pBS (Kintner and Melton, 1987), *Sox2* in pCS2 (Mizuseki et al., 1998), *epidermal keratin* (XK81) in pBS (Jonas et al., 1985). Stained embryos were re-fixed in MEMFA and sectioned at 40 μm with a cryostat.

ACKNOWLEDGMENT

I wish first to thank Professor Naoto Ueno for his exact guidance throughout this study. And I wish to thank Drs. Makoto Mochii, Noriyuki Kinoshita, Hiroki Takahashi, Makoto Nakamura, Takamasa S. Yamamoto, Nobuhiko Mizuno, Masahiro Yuge for helpful advice and discussion, Peter ten Djike for the PS1 antibody and Jun Aruga for cDNA of Zic-related genes. Many thanks are also extended to all the members of Division of Morphogenesis, National Institute for Basic Biology.

This work was carried out at the Division of Morphogenesis, National Institute for Basic Biology.

REFERENCES

Asashima, M., Nakano, H., Shimada, K., Kinoshita, K., Ishii, K., Shibai, H., and Ueno, N. (1990). Mesoderm induction in early amphibian embryos by activin A (erythroid differentiation factor). *Roux's Arch. Dev. Biol.* **198,** 330-335.

Baker, J. C., Beddington, R. S., and Harland, R. M. (1999). Wnt signaling in Xenopus embryos inhibits bmp4 expression and activates neural development. *Genes Dev* **13,** 3149-59.

Barembaum, M., Moreno, T. A., LaBonne, C., Sechrist, J., and Bronner-Fraser, M. (2000). Noelin-1 is a secreted glycoprotein involved in generation of the neural crest. *Nat Cell Biol* **2,** 219-25.

Barth, K. A., Kishimoto, Y., Rohr, K. B., Seydler, C., Schulte-Merker, S., and Wilson, S. W. (1999). Bmp activity establishes a gradient of positional information throughout the entire neural plate. *Development* **126,** 4977-87.

Blitz, I. L., and Cho, K. W. (1995). Anterior neurectoderm is progressively induced during gastrulation: the role of the Xenopus homeobox gene orthodenticle. *Development* **121,** 993-1004.

Carl, T. F., Dufton, C., Hanken, J., and Klymkowsky, M. W. (1999). Inhibition of neural crest migration in Xenopus using antisense slug RNA. *Dev Biol* **213,** 101-15.

Coffman, C. R., Skoglund, P., Harris, W. A., and Kintner, C. R. (1993). Expression of an extracellular deletion of Xotch diverts cell fate in Xenopus embryos. *Cell* **73,**

659-71.

Dale, L., and Jones, C. M. (1999). BMP signalling in early Xenopus development. *Bioessays* **21,** 751-60.

Dosch, R., Gawantka, V., Delius, H., Blumenstock, C., and Niehrs, C. (1997). Bmp-4 acts as a morphogen in dorsoventral mesoderm patterning in Xenopus. *Development* **124,** 2325-34.

Duboule, D. (1994). Guidebook to the Homeobox Genes. *Oxford University Press.*

Dudley, A. T., Lyons, K. M., and Robertson, E. J. (1995). A requirement for bone morphogenetic protein-7 during development of the mammalian kidney and eye. *Genes Dev* **9,** 2795-807.

Dyson, S., and Gurdon, J. B. (1998). The interpretation of position in a morphogen gradient as revealed by occupancy of activin receptors. *Cell* **93,** 557-68.

Ericson, J., Rashbass, P., Schedl, A., Brenner-Morton, S., Kawakami, A., van Heyningen, V., Jessell, T. M., and Briscoe, J. (1997). Pax6 controls progenitor cell identity and neuronal fate in response to graded Shh signaling. *Cell* **90,** 169-80.

Faure, S., Lee, M. A., Keller, T., ten Dijke, P., and Whitman, M. (2000). Endogenous patterns of TGFbeta superfamily signaling during early Xenopus development. *Development* **127,** 2917-31.

Furuta, Y., and Hogan, B. L. M. (1998). BMP4 is essential for lens induction in the mouse embryo. *Genes Dev* **12,** 3764-75.

Gammill, L. S., and Sive, H. (2000). Coincidence of otx2 and BMP4 signaling correlates with Xenopus cement gland formation. *Mech Dev* **92,** 217-26.

Garcia-Castro, M. I., Marcelle, C., and Bronner-Fraser, M. (2002). Ectodermal Wnt function as a neural crest inducer. *Science* **297,** 848-51.

Graff, J. M., Thies, R. S., Song, J. J., Celeste, A. J., and Melton, D. A. (1994). Studies with a Xenopus BMP receptor suggest that ventral mesoderm-inducing signals override dorsal signals in vivo. *Cell* **79,** 169-79.

Hawley, S. H., Wunnenberg-Stapleton, K., Hashimoto, C., Laurent, M. N., Watabe, T., Blumberg, B. W., and Cho, K. W. (1995). Disruption of BMP signals in embryonic Xenopus ectoderm leads to direct neural induction. *Genes Dev* **9,** 2923-35.

Heasman, J. (2002). Morpholino oligos: making sense of antisense? *Dev Biol* **243,** 209-14.

Hogan, B. L. (1996). Bone morphogenetic proteins: multifunctional regulators of vertebrate development. *Genes Dev* **10,** 1580-94.

Iemura, S., Yamamoto, T. S., Takagi, C., Uchiyama, H., Natsume, T., Shimasaki, S., Sugino, H., and Ueno, N. (1998). Direct binding of follistatin to a complex of bone-morphogenetic protein and its receptor inhibits ventral and epidermal cell fates in early Xenopus embryo. *Proc Natl Acad Sci U S A* **95,** 9337-42.

Ikeya, M., Lee, S. M., Johnson, J. E., McMahon, A. P., and Takada, S. (1997). Wnt signalling required for expansion of neural crest and CNS progenitors. *Nature*

389, 966-70.

Irish, V. F., and Gelbart, W. M. (1987). The decapentaplegic gene is required for dorsal-ventral patterning of the Drosophila embryo. *Genes Dev* **1,** 868-79.

Jena, N., Martin-Seisdedos, C., McCue, P., and Croce, C. M. (1997). BMP7 null mutation in mice: developmental defects in skeleton, kidney, and eye. *Exp Cell Res* **230,** 28-37.

Jonas, E., Sargent, T. D., and Dawid, I. B. (1985). Epidermal keratin gene expressed in embryos of Xenopus laevis. *Proc Natl Acad Sci U S A* **82,** 5413-7.

Kim, Y., and Nirenberg, M. (1989). Drosophila NK-homeobox genes. *Proc Natl Acad Sci U S A* **86,** 7716-20.

Kintner, C. R., and Melton, D. A. (1987). Expression of Xenopus N-CAM RNA in ectoderm is an early response to neural induction. *Development* **99,** 311-25.

Kishimoto, Y., Lee, K. H., Zon, L., Hammerschmidt, M., and Schulte-Merker, S. (1997). The molecular nature of zebrafish swirl: BMP2 function is essential during early dorsoventral patterning. *Development* **124,** 4457-66.

Kolm, P. J., and Sive, H. L. (1995). Efficient hormone-inducible protein function in Xenopus laevis. *Dev Biol* **171,** 267-72.

Koshiba-Takeuchi, K., Takeuchi, J. K., Matsumoto, K., Momose, T., Uno, K., Hoepker, V., Ogura, K., Takahashi, N., Nakamura, H., Yasuda, K., and Ogura, T. (2000). Tbx5 and the retinotectum projection. *Science* **287,** 134-7.

LaBonne, C., and Bronner-Fraser, M. (1998). Neural crest induction in Xenopus: evidence for a two-signal model. *Development* **125,** 2403-14.

LaBonne, C., and Bronner-Fraser, M. (2000). Snail-related transcriptional repressors are required in Xenopus for both the induction of the neural crest and its subsequent migration. *Dev Biol* **221,** 195-205.

LeDouarin, N. M., and Kalcheim, C. (1999). The Neural Crest. 2nd edn. *Cambridge University Press, London.*

Lee, K. J., and Jessell, T. M. (1999). The specification of dorsal cell fates in the vertebrate central nervous system. *Annu Rev Neurosci* **22,** 261-94.

Luo, G., Hofmann, C., Bronckers, A. L., Sohocki, M., Bradley, A., and Karsenty, G. (1995). BMP-7 is an inducer of nephrogenesis, and is also required for eye development and skeletal patterning. *Genes Dev* **9,** 2808-20.

Lyons, I., Parsons, L. M., Hartley, L., Li, R., Andrews, J. E., Robb, L., and Harvey, R. P. (1995). Myogenic and morphogenetic defects in the heart tubes of murine embryos lacking the homeo box gene Nkx2-5. *Genes Dev* **9,** 1654-66.

Ma, Q., Chen, Z., del Barco Barrantes, I., de la Pompa, J. L., and Anderson, D. J. (1998). neurogenin1 is essential for the determination of neuronal precursors for proximal cranial sensory ganglia. *Neuron* **20,** 469-82.

Marchant, L., Linker, C., Ruiz, P., Guerrero, N., and Mayor, R. (1998). The inductive properties of mesoderm suggest that the neural crest cells are specified by a BMP gradient. *Dev Biol* **198,** 319-29.

Massague, J., and Wotton, D. (2000). Transcriptional control by the TGF-beta/Smad signaling system. *Embo J* **19,** 1745-54.

Mayor, R., and Aybar, M. J. (2001). Induction and development of neural crest in Xenopus laevis. *Cell Tissue Res* **305,** 203-9.

Mayor, R., Guerrero, N., and Martinez, C. (1997). Role of FGF and noggin in neural crest induction. *Dev Biol* **189,** 1-12.

Mayor, R., Morgan, R., and Sargent, M. G. (1995). Induction of the prospective neural crest of Xenopus. *Development* **121,** 767-77.

McMahon, A. P. (2000). Neural patterning: the role of Nkx genes in the ventral spinal cord. *Genes Dev* **14,** 2261-4.

Mizuseki, K., Kishi, M., Matsui, M., Nakanishi, S., and Sasai, Y. (1998). Xenopus Zic-related-1 and Sox-2, two factors induced by chordin, have distinct activities in the initiation of neural induction. *Development* **125,** 579-87.

Muroyama, Y., Fujihara, M., Ikeya, M., Kondoh, H., and Takada, S. (2002). Wnt signaling plays an essential role in neuronal specification of the dorsal spinal cord. *Genes Dev* **16,** 548-53.

Nakata, K., Koyabu, Y., Aruga, J., and Mikoshiba, K. (2000). A novel member of the Xenopus Zic family, Zic5, mediates neural crest development. *Mech Dev* **99,** 83-91.

Nakata, K., Nagai, T., Aruga, J., and Mikoshiba, K. (1997). Xenopus Zic3, a primary

regulator both in neural and neural crest development. *Proc Natl Acad Sci U S A* **94,** 11980-5.

Nakata, K., Nagai, T., Aruga, J., and Mikoshiba, K. (1998). Xenopus Zic family and its role in neural and neural crest development. *Mech Dev* **75,** 43-51.

Nieuwkoop, P. D., Faber, J. (1967). A Normal Table of Xenopus laevis. *Daudin, North Holland, Amsterdam.*

Nikaido, M., Tada, M., Takeda, H., Kuroiwa, A., and Ueno, N. (1999). In vivo analysis using variants of zebrafish BMPR-IA: range of action and involvement of BMP in ectoderm patterning. *Development* **126,** 181-90.

Nishimatsu, S., Suzuki, A., Shoda, A., Murakami, K., and Ueno, N. (1992). Genes for bone morphogenetic proteins are differentially transcribed in early amphibian embryos. *Biochem Biophys Res Commun* **186,** 1487-95.

Ohkawara, B., Iemura, S., ten Dijke, P., and Ueno, N. (2002). Action range of BMP is defined by its N-terminal basic amino acid core. *Curr Biol* **12,** 205-9.

Persson, U., Izumi, H., Souchelnytskyi, S., Itoh, S., Grimsby, S., Engstrom, U., Heldin, C. H., Funa, K., and ten Dijke, P. (1998). The L45 loop in type I receptors for TGF-beta family members is a critical determinant in specifying Smad isoform activation. *FEBS Lett* **434,** 83-7.

Piccolo, S., Agius, E., Leyns, L., Bhattacharyya, S., Grunz, H., Bouwmeester, T., and De Robertis, E. M. (1999). The head inducer Cerberus is a multifunctional antagonist of Nodal, BMP and Wnt signals. *Nature* **397,** 707-10.

Rohr, K. B., Schulte-Merker, S., and Tautz, D. (1999). Zebrafish zic1 expression in brain and somites is affected by BMP and hedgehog signalling. *Mech Dev* **85,** 147-59.

Sasai, N., Mizuseki, K., and Sasai, Y. (2001). Requirement of FoxD3-class signaling for neural crest determination in Xenopus. *Development* **128,** 2525-36.

Schubert, F. R., Fainsod, A., Gruenbaum, Y., and Gruss, P. (1995). Expression of the novel murine homeobox gene Sax-1 in the developing nervous system. *Mech Dev* **51,** 99-114.

Smith, S. T., and Jaynes, J. B. (1996). A conserved region of engrailed, shared among all en-, gsc-, Nk1-, Nk2- and msh-class homeoproteins, mediates active transcriptional repression in vivo. *Development* **122,** 3141-50.

Spann, P., Ginsburg, M., Rangini, Z., Fainsod, A., Eyal-Giladi, H., and Gruenbaum, Y. (1994). The spatial and temporal dynamics of Sax1 (CHox3) homeobox gene expression in the chick's spinal cord. *Development* **120,** 1817-28.

Spokony, R. F., Aoki, Y., Saint-Germain, N., Magner-Fink, E., and Saint-Jeannet, J. P. (2002). The transcription factor Sox9 is required for cranial neural crest development in Xenopus. *Development* **129,** 421-32.

Suzuki, A., S., N., and Ueno, N. (1995). Bone morphogenetic protein acts as a ventral mesoderm modifier in early Xenopus embryos. *Development Growth and Differentiation* **37,** 581-588.

Suzuki, A., Thies, R. S., Yamaji, N., Song, J. J., Wozney, J. M., Murakami, K., and Ueno,

N. (1994). A truncated bone morphogenetic protein receptor affects dorsal-ventral patterning in the early Xenopus embryo. *Proc Natl Acad Sci U S A* **91,** 10255-9.

Suzuki, A., Ueno, N., and Hemmati-Brivanlou, A. (1997). Xenopus msx1 mediates epidermal induction and neural inhibition by BMP4. *Development* **124,** 3037-44.

Tada, M., O'Reilly, M. A., and Smith, J. C. (1997). Analysis of competence and of Brachyury autoinduction by use of hormone- inducible Xbra. *Development* **124,** 2225-34.

Tanimoto, H., Itoh, S., ten Dijke, P., and Tabata, T. (2000). Hedgehog creates a gradient of DPP activity in Drosophila wing imaginal discs. *Mol Cell* **5,** 59-71.

Wallingford, J. B., and Harland, R. M. (2002). Neural tube closure requires Dishevelled-dependent convergent extension of the midline. *Development* **129,** 5815-25.

Wawersik, S., Purcell, P., Rauchman, M., Dudley, A. T., Robertson, E. J., and Maas, R. (1999). BMP7 acts in murine lens placode development. *Dev Biol* **207,** 176-88.

Wilson, P. A., Lagna, G., Suzuki, A., and Hemmati-Brivanlou, A. (1997). Concentration-dependent patterning of the Xenopus ectoderm by BMP4 and its signal transducer Smad1. *Development* **124,** 3177-84.

Yamamoto, T. S., Takagi, C., Hyodo, A. C., and Ueno, N. (2001). Suppression of head formation by Xmsx-1 through the inhibition of intracellular nodal signaling.

Development **128,** 2769-79.